# Redundant Residue Number System Assisted Multicarrier Direct-Sequence Code-Division Dynamic Multiple-Access for Cognitive Radios

Shuo Zhang, Lie-Liang Yang, *Senior Member, IEEE*, and Youguang Zhang

***Abstract*—A redundant residue number system assisted multicarrier direct-sequence code-division dynamic multiple-access (RRNS MC/DS-CDDMA) scheme is proposed for application in cognitive radios (CRs). Taking the advantages of both the multicarrier direct-sequence code-division multiple-access (MC/DS-CDMA) and the RRNS, the RRNS MC/DS-CDDMA has a low-complexity for implementation, a high-flexibility for reconfiguration and is robust to dynamic spectrums. Associated with the RRNS MC/DS-CDDMA, in this paper, the so-called receiver multiuser diversity aided multi-stage minimum mean-square error multiuser detector (RMD/MS-MMSE MUD) is considered for signal detection. Specifically, three types of RMD/MS-MMSE MUDs are proposed, which are the Type-I.1, Type-II.1 and Type-I.2 RMD/MS-MMSE MUDs. In these MUD schemes, the Type-I.1 MUD carries out the joint detection of all the subcarrier signals using both the observations and the channel state information (CSI) of all the subcarriers. In the Type-I.2 and Type-II.1 RMD/MS-MMSE MUDs, the embedded MMSE-MUDs are implemented subcarrier-by-subcarrier independently. Furthermore, in the Type-I.2 RMD/MS-MMSE MUD, the autocorrelation matrices used by the MMSE-MUDs are free from the CSI. Explicitly, both the Type-II.1 and Type-I.2 RMD/MS-MMSE MUDs are suitable for operation in dynamic spectrum environments. Furthermore, our simulation results show that the above three types of RMD/MS-MMSE MUDs are capable of making the RRNS MC/DS-CDDMA systems achieve similar error and throughput performance. Owing to the above merits, the RRNS MC/DS-CDDMA employing either Type-I.2 or Type-II.1 RMD/MS-MMSE MUD may be considered one of the highly promising DMA schemes for application in CR systems.**

***Index Terms*—Cognitive radios, dynamic multiple-access, multicarrier modulation, code-division multiple-access, residue number system, redundant residue number system, multiuser detection.**

## I. Introduction

Conventional radios are regulated by fixed spectrum allocation policies, which are operated in certain time frames, over certain frequency bands and within certain geographical regions. This fixed spectrum allocation has resulted in low-efficiency in usage of the precious spectrum resources, making most of the allocated (licensed) spectrums are under-utilized. For example, the measurement shows that the average spectrum occupancy from 30 MHz to 3 GHz over six cities is 5.2% and that the maximum total spectrum occupancy is 13.1% in New York City [1]. On the other side, the increasing demand for high-speed wireless multimedia services makes radio spectrum one of the most scarce and valuable resources. Cognitive radios (CRs), which implement opportunistic access of the licensed frequency bands that are under-utilized, have been recognized the possible solutions to the spectrum congestion problem in the future generations of wireless communication systems [2, 3].

According to [4], in CRs, there are four main techniques, including: (1) spectrum sensing for determining available spectrum holes [5] for CR users (CRUs) and for detecting the presence of primary users (PUs), (2) spectrum management motivating to make the spectrum-efficiency as high as possible, (3) spectrum sharing for coordinating the CRUs to access available spectrum and, (4) spectrum mobility for handling the transition from one spectrum to another. Hence, one of the most important issues in CRs is that multiple CRUs access the unused frequency bands and maintain their communications in dynamic frequency environments.

Conceptually, a PU is defined as a licensed user that has preferential right to access the allocated bandwidth. In this paper, we assume that the PUs and CRUs are operated in the interweave paradigm [6], where CRUs can only communicate opportunistically on the spectrums not occupied by PUs and without causing degradation of PUs' quality of services (QoS). Once there are PUs appearing on some spectrums being used by some CRUs, these CRUs must vacate the corresponding spectrums and move to some others, whenever available. This process is usually referred to as spectrum handoff. Explicitly, for spectrum handoff, the CRs require time to acquire the knowledge about the available spectrums, the corresponding channel state information (CSI), etc., and to restructure the CRUs to make efficiently use of the newly available spectrums. Hence, in order to maintain seamless communications, a CR system is expected to be robust to spectrum varying and have a high-flexibility for on-line reconfiguration.

Motivated by the above concerns, in [7], we have proposed a dynamic multiple-access (DMA) scheme for making use of the time-varying spectrums in CR systems. Our DMA scheme is designed by taking the advantages of both the multicarrier direct-sequence code-division multiple-access (MC/DS-CDMA) [8–11] and the redundant residue number system (RRNS) [12–16], which is referred to as the RRNS MC/DS-

 S. Zhang and Y. Zhang are with the School of Electronic and Information Engineering, Beihang University, Beijing 100191, China. (E-mail: gcshuo@gmail.com, zhangyouguang@vip.sina.com). L.-L. Yang is with School of Electronics and Computer Science, University of Southampton, SO17 1BJ, UK. (E-mail: lly@ecs.soton.ac.uk). This work was presented in part at the IEEE VTC2011 Spring, 15-18 May, 2011, Budapest, Hungary.

CDDMA for convenience of description in the following texts. The advantages of the MC/DS-CDMA and the RRNS can be briefly summarized as follows. First, it has been well-recognized that the MC/DS-CDMA scheme has the highest flexibility and highest number of degrees-of-freedom for reconfigurations [8], which may render the RRNS MC/DS-CDDMA a versatile multiple access scheme that is suitable for CR systems. The MC/DS-CDMA scheme is also beneficial to pseudo-noise (PN) sequence acquisition, in comparison with the single-carrier DS-CDMA [17–19]. Second, the signal processing based on RRNS has a range of advantages that are beneficial to DMA [12–14]. RRNS-based arithmetics exhibit a modular structure that leads naturally to parallelism in digital hardware. Comparing with the conventional weighted number systems, such as the binary weighted number system representation, the RRNS has two attractive inherent features [12, 14]: (a) the carry-free arithmetic and (b) the lack of ordered significance among the residues. The first property implies that the operations related to the different residues of the RRNS are mutually independent. The second property implies that any erroneous residues may be discarded without affecting the data recovery, provided that a sufficient dynamic range remains in the reduced RRNS in order to unambiguously represent the non-redundant information. Due to the above-mentioned properties of both the MC/DS-CDMA and the RRNS, our proposed RRNS MC/DS-CDDMA is well suitable for DMA in CRs environments.

In this paper, we focus on design of low-complexity, high-efficiency and high-flexibility multiuser detection (MUD) schemes for the RRNS MC/DS-CDDMA systems, and on studying the achievable error and throughput performance of the RRNS MC/DS-CDDMA systems employing the proposed MUD algorithms. Three types of MUD schemes are designed based on the principles of the receiver multiuser diversity aided multi-stage minimum mean-square error MUD (RMD/MS-MMSE MUD) [20–23], yielding the so-called Type-I.1, Type-I.2 and Type-II.1 RMD/MS-MMSE MUDs. Specifically, the Type-I.1 MUD carries out the joint detection of all the subcarrier signals using both the observations and the channel state information (CSI) associated with all the subcarriers. By contrast, in the both the Type-I.2 and Type-II.1 RMD/MS-MMSE MUDs, the embedded MMSE-MUDs are implemented subcarrier-by-subcarrier independently. Furthermore, in the Type-I.2 RMD/MS-MMSE MUD, the autocorrelation matrices used by the corresponding MMSE-MUDs are not dependent on any CSI. Hence, their inverse matrices are required to be updated, only when the active CRUs change. Therefore, from the Type-I.1 to the Type-II.1 and, finally, to the Type-I.2 RMD/MS-MMSE MUD, the implementation complexity becomes lower and lower while the implementation flexibility becomes higher and higher. In this paper, the error and throughput performance of the RRNS MC/DS-CDDMA systems employing the proposed MUD schemes are investigated, when assume communications over frequency-selective fading channels. From the performance results, we observe that the three types of RMD/MS-MMSE MUDs are capable of making the RRNS MC/DS-CDDMA systems achieve similar error and throughput performance. Owing to the above properties, we can argue that the RRNS MC/DS-CDDMA employing either Type-I.2 or Type-II.1 RMD/MS-MMSE MUD constitutes one of the highly promising DMA schemes for application in CR systems. Note that, in [7], the performance of the RRNS/MC DS-CDDMA systems has been investigated, when a so-called suboptimum MMSE interference cancellation (SMMSE-IC) scheme is employed.

The reminder of this paper is organized as follows. Section II describes the main assumptions for the PR and CR systems. In Section III, the RRNS MC/DS-CDDMA system model is addressed, while, in Section IV, the three types of RMD/MS-MMSE MUD schemes are detailed. In Section V, we derive the outage probability and the lower bound error probability of the RRNS MC/DS-CDDMA systems. Section VI provides performance results and discussion and, finally, in Section VII, we summarize the main conclusions.

## II. Operational Models of Primary and Cognitive Radio Systems

In this paper, we assume that the PUs and CRUs are operated under the interweave paradigm [6]. In this case, the CRUs are only allowed to communicate opportunistically on the spectrums not occupied by the PUs, which are usually referred to as the ‘spectrum holes’, without disturbing the PUs’ communication and affecting their QoS. A CRU communicating on a given spectrum band must terminate its communication, once the band is found to be used by PUs.

In order to carry out the related investigation, in this paper, we assume that the whole frequency band accessible by the CRUs is divided into $C$ subbands supported by the corresponding subcarriers. The $C$ subbands are allocated to support maximal $K_P$ number of PUs. Once a PU becomes active, it is assumed to occupy $C_P$ subbands, where we assume that $K_pC_P \leq C$. We assume that the PUs activate according to the $M/M/K_P/K_P/K_P$ queuing model [24]. In this $M/M/K_P/K_P/K_P$ queuing model, the number of active PUs follows a Poisson distribution associated with an arrival rate $\lambda$, the service time obeys a negative exponential distribution with mean $1/\mu$, and the number of servers, system capacity as well as the total number of customers are the same and have a value of $K_P$ [24, 25]. According to the queuing theory [25], after the system converges to its steady state, the probability of the event that there are $n$ active PUs is

$$P_0 = \left[K_P! \sum_{i=0}^{K_P} \frac{1}{(K_P-i)!i!}\left(\frac{\lambda}{\mu}\right)^i\right]^{-1},$$
$$P_n = \frac{K_P!}{(K_P-n)!n!}\left(\frac{\lambda}{\mu}\right)^n P_0,\ 1 \leq n \leq K_P \quad (1)$$

Based on the above assumptions for the PRs, we can know that the frequency bands possible for the CR system are dynamic. The number of subbands available for the CRUs is given by

$$\bar{C} = C - nC_P,\ n = 0, 1, \ldots, K_P \quad (2)$$

when there are $n$ active PUs, where $n$ may take any value in $\{0, 1, \ldots, K_p\}$ with the probabilities given in (1).

Let us assume that the channels assigned to an active PU are uniformly and randomly chosen from the unused frequency subbands. In this case, the subbands available for the CRUs also constitute a Poisson process with its parameters that can be readily derived from the corresponding PUs' Poisson process [25]. We assume that the CRUs have the same priority to access the $\bar{C}$ subbands based on the RRNS MC/DS-CDDMA scheme that will be detailed in our forthcoming discourse. Furthermore, when the CRUs are capable of accessing all the $\bar{C}$ subbands provided by the above $M/M/K_P/K_P/K_P$ queuing model without any other limitations, we say that the CR system is operated under the *ideal mode*. However, in practice when operated under the interweave paradigm [6], some other constraints are usually imposed on the CR systems accessing the frequency spectrum. For example, a CR must immediately clear the being used subbands, once it realizes that the subbands are occupied by PUs. Therefore, for the sake of distinction, we refer to this constraint operational scenario as the *constraint mode*.

Specifically, in this paper, our proposed RRNS MC/DS-CDDMA is considered to be operated under the constraint mode by taking into account the effect of spectrum handoff, which is referred to as the *handoff mode*. The operations under the handoff mode are as follows. Let us assume that there are $n$ active PUs at $t$. After a time duration of $\Delta t$, some of the $(K_P - n)$ inactive PUs may become active to start communication. The probability that $i$ out of the $(K_P - n)$ inactive PUs become active within $\Delta t$ is given by [25]

$$P'_i = \frac{[\lambda(K_P - n)\Delta t]^i}{i!} e^{-\lambda(K_P-n)\Delta t}, \quad i = 0, 1 \ldots, K_P - n \tag{3}$$

Additionally, once CRUs realize that there are 'new' PUs appearing on some of the subbands they occupy, the CRUs immediately terminate their communications on these subbands. Simultaneously, after a time duration of $\Delta t$, some active PUs may complete their communications and become idle. The probability of the event that $k$ active PUs become inactive within $\Delta t$ is given by [25]

$$\bar{P}'_k = n\mu\Delta t e^{-n\mu(k\Delta t)}, \; k = 0, 1, \ldots. \tag{4}$$

In this case, there will be some new subbands available for the CRUs. However, the CR systems have to sense the spectrum first and also need to estimate the channels of the newly found subbands found, in order to access them. These processes should take some time. Therefore, the spectrum handoff may impose a significant impact on the achievable performance of the CR systems, if the DMA scheme is not efficiently designed. In order to avoid communication interruption, an efficient DMA scheme should offer sufficient time for spectrum handoff and can tolerate some loss of signals. Motivated by these issues, our RRNS MC/DS-CDDMA systems take into account of the spectrum handoff. As demonstrated in the forthcoming discourses, the RRNS techniques make the CRUs robust to the spectrum varying and allow to implement seamless spectrum handoff.

## III. Description of RRNS MC/DS-CDDMA Systems

### *A. A Brief Overview of RNS and RRNS*

A residue number system (RNS) is defined [12] by a set of, say $S$, positive integers denoted by $m_1, m_2, \ldots, m_S$, which are referred to as information moduli. All the moduli are pairwise relative primes. In this RNS, any integer $0 \leq X < M_I = \prod_{s=1}^{S} m_s$ can be uniquely and unambiguously represented by a residue sequence $(r_1, r_2, ..., r_S)$, where $r_s = X \mod m_s$ represents the residue of $X$ with respect to $m_s$ and $0 \leq r_s < m_s$. Reversely, in this RNS, given an $S$-tuple residue sequence $(r_1, r_2, ..., r_S)$ with $0 \leq r_s < m_s, \; s = 1, ..., S$, according to the Chinese reminder theorem (CRT) [26], there exists one and only one integer $0 \leq X < M_I$ satisfying $r_s = X \mod m_s$. In other words, if $(r_1, r_2, ..., r_S)$ conveys a message $X$, it can be recovered uniquely and unambiguously with the aid of, for example, the CRT.

For the sake of incorporating error control or making a RNS-based system fault-tolerant, redundant moduli can be appended to the information moduli, forming the so-called redundant residue number system (RRNS) [12, 15, 26–28]. Specifically, $(Q - S)$ moduli $m_{S+1}, m_{S+2}, ..., m_Q$, referred to as redundant moduli, can be added to the previously introduced RNS, in order to form a RRNS with $Q$ positive, pairwise relative prime integers. Usually, it is required that $\min\{m_{S+1}, m_{S+2}, ..., m_Q\} > \max\{m_1, m_2, \ldots, m_S\}$. Let the product of $m_{S+1}, m_{S+2}, ..., m_Q$ be denoted by $M_R$. Now in the RRNS, an integer $X$ in the range $[0, M_I)$ can be represented by an $Q$-tuple residue sequence $(r_1, r_2, ..., r_Q)$ with respect to the $Q$ moduli of the RRNS. At the receiver, based on $(r_1, r_2, ..., r_Q)$, the RRNS decoding processing, such as erasure-only decoding, error-correction-only decoding or error-and-erasure decoding [27, 28], may be implemented to recover the message $X$.

In this paper, our RRNS MC/DS-CDDMA system is designed based on the principles of RRNS, which is now described as follows.

### *B. Transmitter*

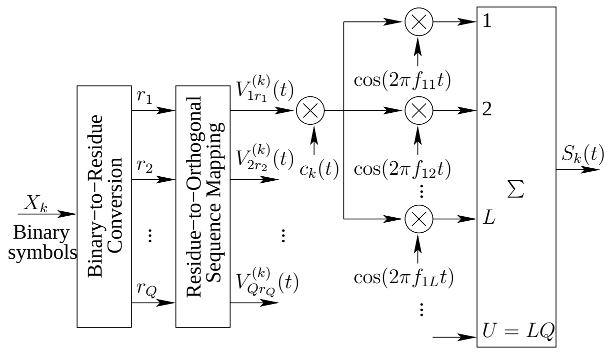


Fig. 1. Transmitter schematic block diagram of the $k$th CRU in the RRNS MC/DS-CDDMA system.

The transmitter schematic block diagram for the $k$th CRU is shown in Fig. 1. The binary bits to be transmitted are first transformed to a residue sequence $(r_1^{(k)}, r_2^{(k)}, ..., r_Q^{(k)})$, which represents a message having the integer value $0 \leq X_k < M$, where $M \leq M_I (= \prod_{s=1}^{S} m_s)$ and usually takes a value in the form of $2^B$ with $B$ denoting the number of bits per symbol. Then, the $Q$ residues are mapped to $Q$ number of orthogonal sequences based on the $M$-ary orthogonal-shift keying (MOSK) principles [29]. In this paper, orthogonal Hadamard-Walsh codes are assumed, and every CRU is assigned the same set of orthogonal sequences consisting of $\sum_{q=1}^{Q} m_q$ orthogonal Hadamard-Walsh codes of length $N_s$, arranged as:

$$\left\{ \begin{array}{c} V_{10}(t), V_{11}(t), ..., V_{1(m_1-1)}(t); \\ V_{20}(t), V_{21}(t), ..., V_{2(m_2-1)}(t); \\ \cdots\cdots \\ V_{Q0}(t), V_{Q1}(t), ..., V_{Q(m_Q-1)}(t) \end{array} \right\} \tag{5}$$

where the subset $\{V_{q0}(t), V_{q1}(t), ..., V_{q(m_q-1)}(t)\}$, $q = 1, \ldots, Q$, is for transmission of the residue $r_q^{(k)}$, $k = 1, \ldots, K$, by taking one out of the $m_q$ orthogonal codes according to the value of $r_q^{(k)}$. Note that, owing to the orthogonality of the subcarriers in the RRNS MC/DS-CDDMA, some of the orthogonal codes in the different rows of (5) can be the same. Let $N_s = T_s/T_r$, where $T_s$ denotes the symbol interval and $T_r$ is the duration of the orthogonal codes' waveforms, referred to as *fraction* for convenience. Then, the orthogonal code waveform can be expressed as $V_{qr_q}^{(k)}(t) = \sum_{n=0}^{N_s-1} V_{qr_q}^{(k)}[n] P_{T_r}(t - nT_r)$, where $V_{qr_q}^{(k)}[n] = \pm 1$, $P_{T_r}(t)$ represents the rectangular waveform of duration $T_r$. As shown in Fig. 1, after the mapping from residues to orthogonal sequences, each of the $Q$ orthogonal sequences is spread by a user specific signature sequence. Furthermore, each of the $Q$ spreading sequences is transmitted on $L$ subcarriers, in order to achieve an $L$th order frequency diversity. Therefore, the RRNS MC/DS-CDDMA system requires a total $U = LQ$ number of subcarriers. Specifically, according to Fig. 1, the transmitted signal by CRU $k$ can be expressed as

$$S_k(t) = \sum_{q=1}^{Q} \sum_{l=1}^{L} \sqrt{\frac{2P}{U}} V_{qr_q}^{(k)}(t) c_k(t) \cos(2\pi f_{ql} t + \phi_{ql}^{(k)}), \quad k = 1, 2, \ldots, K \tag{6}$$

where $P$ is the total transmission power of the $U$ number of subcarriers, $c_k(t)$ represents the spreading code assigned to the $k$th CRU, which can be expressed as $c_k(t) = \sum_{j=0}^{\infty} c_j^{(k)} \psi(t - jT_c)$, where $c_j^{(k)}$ assumes a value of $+1$ or $-1$, while $\psi(t)$ is the chip-waveform of the spreading sequences, which is normalized to satisfy $\int_0^{T_c} \psi^2(t) dt = T_c$. Furthermore, we define $N_e = T_r/T_c$, which is the number of chips per fraction. Finally, in (6), $\phi_{ql}^{(k)}$ represents the initial phase associated with the subcarrier $f_{ql}$.

### C. Receiver

We assume that there are $K$ CRUs using the same $U = LQ$ number of subcarriers to communicate with one CR base-station (CRBS). The subcarrier channels from the $K$ CRUs to the CRBS are assumed to experience flat fading. Furthermore, we assume synchronous transmission and ideal power-control among the CRUs. Then, the received baseband equivalent signal at the CRBS can be expressed as

$$R(t) = \sum_{k=1}^{K} \sum_{q=1}^{Q} \sum_{l=1}^{L} \sqrt{\frac{2P}{U}} h_{ql}^{(k)} V_{qr_q}^{(k)}(t) c_k(t) \exp(j2\pi f_{ql} t) + n(t) \tag{7}$$

where $h_{ql}^{(k)}$ represents the channel gain of the $ql$th subcarrier of the $k$th CRU, which obeys the independent identically distributed (iid) complex Gaussian distribution with zero mean and a variance $0.5$ per dimension. In (7), $n(t)$ denotes the complex baseband equivalent Gaussian noise, which has zero mean and a single-sided power-spectrum density (PSD) of $N_0$ per dimension. Note that, without loss of generality, in (7), the initial phases due to subcarrier modulations at the CRUs were absorbed into the channel gains. Additionally, the $ql$th subcarrier is the one determined by the indexes $q$ and $l$.

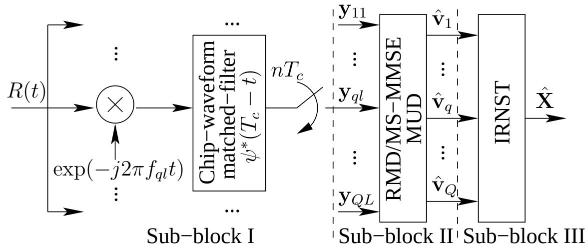


Fig. 2. Receiver schematic block diagram for the RRNS MC/DS-CDDMA system.

The receiver schematic block diagram for the RRNS MC/DS-CDDMA is shown as Fig. 2. The receiver can be virtually divided into three sub-blocks. In Sub-block I, the multicarrier demodulation is first executed. We assume that the subcarrier signals are configured so that the subcarrier signals are orthogonal with each other at chip-level [30], which hence do not conflict inter-carrier interference (ICI). Then, a chip waveform matched-filter (MF) with its time domain impulse response $\psi^*(T_c - t)$ is employed by each of the $U$ subcarrier branches. As shown in Fig. 2, the chip waveform MFs' outputs are sampled at the chip-rate in order to provide the discrete observations for detection. It can be shown that the $n$th observation in the $n_s$th fraction of $V_{qr_q}^{(k)}(t)$ and the $ql$th subcarrier can be expressed as

$$y_{ql,n}[n_s] = \frac{1}{\sqrt{2PN_sN_e}T_c} \int_{n_sT_r+nT_c}^{n_sT_r+(n+1)T_c} R(t) \times \psi^*(t) \exp(-j2\pi f_{ql} t) dt \tag{8}$$

where the factor of $1/(\sqrt{2PN_sN_e}T_c)$ is for normalization. When substituting (7) into the above equation, we obtain

$$y_{ql,n}[n_s] = \sum_{k=1}^{K} \frac{1}{\sqrt{N_sN_eU}} h_{ql}^{(k)} c_{n_sN_s+n}^{(k)} V_{qr_q}^{(k)}[n_s] + N_{ql,n}[n_s], \quad q = 1, 2, ..., Q;\ l = 1, 2, ..., L; \quad n_s = 0, 1, \ldots, N_s - 1;\ n = 0, 1, ..., N_e - 1 \tag{9}$$

where $N_{ql,n}[n_s]$ represents the sampled noise, which obeys the Gaussian distribution with zero mean and a variance of $\sigma^2/2 =$

$1/(2\gamma_s)$ per dimension, where $\gamma_s = E_s/N_0$ denotes the signal-to-noise ratio (SNR) per symbol and $E_s = PT_s$ denotes the energy per (RRNS) symbol. Furthermore, let $B = \log_2 M$ be the number of bits conveyed by every RRNS symbol. Then, we have $\gamma_s = B\gamma_b$ with $\gamma_b$ representing the SNR per bit.

As shown in Fig. 2, after the processing in Sub-block I, the observations are sent to the Sub-block II, where multiuser detection (MUD) is carried out to suppress the multiuser interference (MUI). Finally, after the inverse RNS transform (IRNST) by Sub-block III, the information transmitted by the $K$ CRUs is recovered. Let us consider the operations of Sub-blocks II and III of Fig. 2 in the following sections.

## IV. Signal Detection in RRNS MC/DS-CDDMA Systems

From the description of the RRNS MC/DS-CDDMA systems in Section III, we can know that the RRNS MC/DS-CDDMA signals conflict MUI and channel fading, in addition to Gaussian noise, as explicitly seen in (9). Channel fading can be mitigated with the aid of the frequency-diversity attained by transmitting every residue digit over multiple subcarrier channels experiencing independent fading. However, in multiuser systems, diversity scheme becomes efficient only after the MUI is sufficiently suppressed. Otherwise, the performance improvement contributed by the diversity will be overwhelmed by the performance degradation generated by the MUI. Furthermore, when operated in dynamic communication environments, low-complexity detection is critical. Considering these issues, in this contribution, we extend the RMD/MS-MMSE MUD proposed in [20–23] to the RRNS MC/DS-CDDMA systems. As the studies in [20, 22, 23] show, the RMD/MS-MMSE MUD is a low-complexity and high-efficiency MUD scheme, which is capable of achieving the near single-user error performance, even when the multiuser systems are full-load, where the number of active users is equal to the spreading factor. Specifically, for our RRNS MC/DS-CDDMA, the RMD/MS-MMSE MUD is operated at the fraction level to suppress the MUI. Then, MOSK demodulation is carried out to recover the $Q$ moduli transmitted and, finally, the information symbol represented by the RRNS is recovered by the IRNST. Note that, the detectors considered below are all the coherent detection schemes, which require both the channel knowledge of all the CRUs and the knowledge about the PN sequences used by all the CRUs. The channel knowledge may be obtained with the aid of the advanced time/frequency-domain channel estimation [31, 32], while the PN sequences can be acquired by the algorithms proposed, such as, in [17–19, 33, 34]. In this paper, since our focus is on the RRNS/MC DS-CDDMA as well as its achievable performance, we hence assume that the channel knowledge is ideal and all the PN sequences are ideally known to the receiver.

### A. Fraction Level RMD/MS-MMSE MUD

Let us define

$$\begin{aligned}
\boldsymbol{v}_q[n_s] &= \frac{1}{\sqrt{N_s}}\left[V_{qr_q}^{(1)}[n_s], V_{qr_q}^{(2)}[n_s], \cdots, V_{qr_q}^{(K)}[n_s]\right]^T,\\
\boldsymbol{y}_{ql}[n_s] &= [y_{ql,0}[n_s], y_{ql,1}[n_s], \cdots, y_{ql,N_e-1}[n_s]]^T,\\
\boldsymbol{n}_{ql}[n_s] &= [N_{ql,0}[n_s], N_{ql,1}[n_s], \cdots, N_{ql,N_e-1}[n_s]]^T,\\
\boldsymbol{c}_k[n_s] &= \frac{1}{\sqrt{N_e}}[c_{n_sN_s}^{(k)}, c_{n_sN_s+1}^{(k)}, \cdots, c_{n_sN_s+N_e-1}^{(k)}]^T,\\
\boldsymbol{C}[n_s] &= [\boldsymbol{c}_1[n_s], \boldsymbol{c}_2[n_s], \cdots, \boldsymbol{c}_K[n_s]], \qquad (10)\\
\bar{\boldsymbol{H}}_{ql} &= \frac{1}{\sqrt{U}}\text{diag}\left\{h_{ql}^{(1)}, h_{ql}^{(2)}, \cdots, h_{ql}^{(K)}\right\}\\
\boldsymbol{H}_{ql}[n_s] &= \boldsymbol{C}[n_s] \times \bar{\boldsymbol{H}}_{ql}
\end{aligned}$$

Then, it can be shown that

$$\begin{aligned}
\boldsymbol{y}_{ql}[n_s] =& \boldsymbol{H}_{ql}[n_s]\boldsymbol{v}_q[n_s] + \boldsymbol{n}_{ql}[n_s],\ n_s = 0, 1, \ldots, N_s - 1;\\
& q = 1, \ldots, Q;\ l = 1, \ldots, L \qquad (11)
\end{aligned}$$

Furthermore, let

$$\begin{aligned}
\boldsymbol{y}_q[n_s] &= \left[\boldsymbol{y}_{q1}^T[n_s], \boldsymbol{y}_{q2}^T[n_s], \cdots, \boldsymbol{y}_{qL}^T[n_s]\right]^T\\
\boldsymbol{H}_q[n_s] &= \left[\boldsymbol{H}_{q1}^T[n_s], \boldsymbol{H}_{q2}^T[n_s], \cdots, \boldsymbol{H}_{qL}^T[n_s]\right]^T \qquad (12)\\
\boldsymbol{n}_q[n_s] &= \left[\boldsymbol{n}_{q1}^T[n_s], \boldsymbol{n}_{q2}^T[n_s], \cdots, \boldsymbol{n}_{qL}^T[n_s]\right]^T
\end{aligned}$$

Then, we can write

$$\begin{aligned}
\boldsymbol{y}_q[n_s] = \boldsymbol{H}_q[n_s]\boldsymbol{v}_q[n_s] + \boldsymbol{n}_q[n_s],\ n_s = 0, 1, \ldots, N_s - 1;\\
q = 1, \ldots, Q \qquad (13)
\end{aligned}$$

Additionally, if we express

$$\begin{aligned}
\boldsymbol{H}_{ql}[n_s] &= \left[\boldsymbol{h}_{ql}^{(1)}[n_s], \boldsymbol{h}_{ql}^{(2)}[n_s], \cdots, \boldsymbol{h}_{ql}^{(K)}[n_s]\right]\\
\boldsymbol{H}_q[n_s] &= \left[\boldsymbol{h}_q^{(1)}[n_s], \boldsymbol{h}_q^{(2)}[n_s], \cdots, \boldsymbol{h}_q^{(K)}[n_s]\right] \qquad (14)
\end{aligned}$$

Then, it can be shown that $\boldsymbol{y}_{ql}[n_s]$ and $\boldsymbol{y}_q[n_s]$ can be represented as

$$\boldsymbol{y}_{ql}[n_s] = \sum_{k=1}^{K}\boldsymbol{h}_{ql}^{(k)}[n_s]v_q^{(k)}[n_s] + \boldsymbol{n}_{ql}[n_s] \qquad (15)$$

$$\boldsymbol{y}_q[n_s] = \sum_{k=1}^{K}\boldsymbol{h}_q^{(k)}[n_s]v_q^{(k)}[n_s] + \boldsymbol{n}_q[n_s] \qquad (16)$$

In (15) and (16), $v_q^{(k)}[n_s] = V_{qr_q}^{(k)}[n_s]/\sqrt{N_s}$ is the $k$th entry of $\boldsymbol{v}_q[n_s]$, which is the $n_s$th fraction of the orthogonal code transmitted by the $k$th CRU.

The RMD/MS-MMSE MUDs considered below are derived based on (11) - (16) in correspondence with the different scenarios, which have different complexity requirements. For the sake of distinction, we classify them as the Type-I and Type-II RMD/MS-MMSE MUDs. Furthermore, Type-I includes Type-I.1 and Type-I.2 and Type-II includes Type-II.1 and Type-II.2, which will become explicit by following the discussion below.

According to [20–22], the RMD/MS-MMSE MUD is an iterative MUD, which iteratively carries out the operations of MMSE-MUD, identifying and detecting the most reliable CRU and interference cancellation (IC), until all the CRUs are detected. Below we first analyze the component MMSE-MUD and reliability measurement (RM), before stating the RMD/MS-MMSE MUD algorithm.

*1) MMSE-MUD:* The Type-I RMD/MS-MMSE MUD is built on (13) or (16). Its related MMSE-MUD forms the decision variable vector as

$$\hat{\boldsymbol{v}}_q[n_s] = \Re\left\{\boldsymbol{W}_q^H[n_s]\boldsymbol{y}_q[n_s]\right\},\ n_s = 0, 1, \ldots, N_s - 1;\quad q = 1, \ldots, Q \tag{17}$$

where

$$\boldsymbol{W}_q[n_s] = \boldsymbol{R}_{\boldsymbol{y}_q}^{-1}[n_s]\boldsymbol{R}_{\boldsymbol{y}_q\boldsymbol{v}_q}[n_s], \tag{18}$$

$\boldsymbol{R}_{\boldsymbol{y}_q}[n_s]$ and $\boldsymbol{R}_{\boldsymbol{y}_q\boldsymbol{v}_q}[n_s]$ are the autocorrelation matrix of $\boldsymbol{y}_q[n_s]$ and the cross-correlation matrix between $\boldsymbol{y}_q[n_s]$ and $\boldsymbol{v}_q[n_s]$, respectively. With the definitions in (10) and (12), the autocorrelation matrix is given by

$$\begin{aligned}\boldsymbol{R}_{\boldsymbol{y}_q}[n_s] =& E\left[\boldsymbol{y}_q[n_s]\boldsymbol{y}_q^H[n_s]\right] = \frac{1}{N_s}\boldsymbol{H}_q[n_s]\boldsymbol{H}_q^H[n_s] + \sigma^2\boldsymbol{I}_{LN_e}\\ =& \frac{1}{N_s}\sum_{k=1}^{K}\boldsymbol{h}_q^{(k)}[n_s]\left(\boldsymbol{h}_q^{(k)}[n_s]\right)^H + \sigma^2\boldsymbol{I}_{LN_e}\end{aligned} \tag{19}$$

where $\boldsymbol{I}_{LN_e}$ denotes an $(LN_e \times LN_e)$ identity matrix. In (19), $\boldsymbol{R}_{\boldsymbol{y}_q}[n_s]$ is an $(LN_e \times LN_e)$ Hermitian matrix that is channel-dependent. Hence, it is needed to be updated according to the time-varying of the fading channels experienced. This type of autocorrelation matrix can be obtained using relatively short-range average of the observations at the receiver. The RMD/MS-MMSE MUD invoking the autocorrelation matrix of channel-dependent, as shown in the form of (19), is classified as the Type-I.1 RMD/MS-MMSE MUD.

In order to reduce the detection complexity, relatively long-range average may be used to obtain the autocorrelation matrix $\boldsymbol{R}_{\boldsymbol{y}_q}[n_s]$ of channel-independent. In this case, after averaging out the channels in (19), we obtain

$$\boldsymbol{R}_{\boldsymbol{y}_q}[n_s] = \left(\boldsymbol{I}_L \otimes \frac{1}{UN_s}\boldsymbol{C}[n_s]\boldsymbol{C}^T[n_s]\right) + \sigma^2\boldsymbol{I}_{LN_e} \tag{20}$$

where $\otimes$ denotes the *Kronecker production* operation. The RMD/MS-MMSE MUD making use of the channel-independent autocorrelation matrix in the form of (20) is referred to as the Type-I.2 RMD/MS-MMSE MUD.

Note that, if the spreading codes assigned to the $K$ users are fraction independent or, in other words, if $\boldsymbol{C}[n_s]$ is independent of the index $n_s$, then, both (19) and (20) will be independent of the index $n_s$. Explicitely, by doing this the complexity of the corresponding RMD/MS-MMSE MUD can be further reduced, since the autocorrelation matrix invoked is only required to be computed once for all the $N_s$ fractions.

In (18), the cross-correlation matrix for either the Type-I.1 or Type-I.2 is given by

$$\boldsymbol{R}_{\boldsymbol{y}_q\boldsymbol{v}_q}[n_s] = E\left[\boldsymbol{y}_q[n_s]\boldsymbol{v}_q^H[n_s]\right] = \frac{1}{N_s}\boldsymbol{H}_q[n_s] \tag{21}$$

Therefore, for the Type-I.1 RMD/MS-MMSE MUD, after substituting (19) and (21) into (18), we obtain

$$\boldsymbol{W}_q[n_s] = \left(\boldsymbol{H}_q[n_s]\boldsymbol{H}_q^H[n_s] + N_s\sigma^2\boldsymbol{I}_{LN_e}\right)^{-1}\boldsymbol{H}_q[n_s] \tag{22}$$

which needs to invert an $(LN_e \times LN_e)$ matrix of channel dependent. Similarly, for the Type-I.2 RMD/MS-MMSE MUD, after substituting (20) and (21) into (18), we obtain

$$\boldsymbol{W}_q[n_s] = \left[\left(\boldsymbol{I}_L \otimes \frac{1}{U}\boldsymbol{C}[n_s]\boldsymbol{C}^T[n_s]\right) + N_s\sigma^2\boldsymbol{I}_{LN_e}\right]^{-1}\boldsymbol{H}_q[n_s] \tag{23}$$

Furthermore, in (23), if we let $\boldsymbol{W}_q[n_s] = [\boldsymbol{W}_{q1}[n_s], \boldsymbol{W}_{q2}[n_s], \cdots, \boldsymbol{W}_{qL}[n_s]]^T$, then, with the aid of (12), it can be shown that

$$\boldsymbol{W}_{ql}[n_s] = \left[\frac{1}{U}\boldsymbol{C}[n_s]\boldsymbol{C}^T[n_s] + N_s\sigma^2\boldsymbol{I}_{N_e}\right]^{-1}\boldsymbol{H}_{ql}[n_s],\quad l = 1, 2, \ldots, L \tag{24}$$

where the inversion operation is channel independent. Equation (24) explains that, during the whole detection procedure, the Type-I.2 RMD/MS-MMSE MUD needs to invert $N_s$ number of $(N_e \times N_e)$ matrices once, if $\boldsymbol{C}[n_s]$ is dependent on $n_s$. If $\boldsymbol{C}[n_s]$ is independent of $n_s$, then, the RMD/MS-MMSE MUD only needs to invert an $(N_e \times N_e)$ matrix once during the whole detection procedure.

Upon substituting (24) into (17), the decision variable vector for $\boldsymbol{v}_q[n_s]$ can be simplified to

$$\hat{\boldsymbol{v}}_q[n_s] = \Re\left\{\sum_{l=1}^{L}\boldsymbol{W}_{ql}^H[n_s]\boldsymbol{y}_{ql}[n_s]\right\},\quad n_s = 0, 1, \ldots, N_s - 1;\ q = 1, \ldots, Q \tag{25}$$

which implies that the related MMSE-MUDs associated with the $U$ subcarriers are independent. Explicitly, this property is highly beneficial to the DMA in CR systems, since in these systems the frequency bands are time-varying. In this case, once some frequency bands are removed from a CR system or some new frequency bands are added to a CR system, the CR system only needs to deal with the corresponding subcarriers covered by the frequency bands switched off or turned on, without affecting the operations of the other subcarriers.

Against the above observation, the Type-II RMD/MS-MMSE MUDs are directly designed to achieve the subcarrier-by-subcarrier independent detection based on (11) or (15). Correspondingly, the decision variable vectors formed by the related MMSE-MUDs are given by

$$\hat{\boldsymbol{v}}_q[n_s] = \Re\left\{\sum_{l=1}^{L}\bar{\boldsymbol{W}}_{ql}^H[n_s]\boldsymbol{y}_{ql}[n_s]\right\},\quad n_s = 0, 1, \ldots, N_s - 1;\ q = 1, \ldots, Q \tag{26}$$

where the weight matrices are given by

$$\bar{\boldsymbol{W}}_{ql}[n_s] = \boldsymbol{R}_{\boldsymbol{y}_{ql}}^{-1}[n_s]\boldsymbol{R}_{\boldsymbol{y}_{ql}\boldsymbol{v}_q}[n_s],\ n_s = 0, 1, \ldots, N_s - 1;\quad q = 1, 2, \ldots, Q;\ l = 1, 2, \ldots, L \tag{27}$$

The autocorrelation matrix for the Type-II.1 RMD/MS-MMSE MUD is

$$\begin{aligned}\boldsymbol{R}_{\boldsymbol{y}_{ql}}[n_s] &= E\left[\boldsymbol{y}_{ql}[n_s]\boldsymbol{y}_{ql}^H[n_s]\right] = \frac{1}{N_s}\boldsymbol{H}_{ql}[n_s]\boldsymbol{H}_{ql}{}^H[n_s] + \sigma^2\boldsymbol{I}_{N_e}\\ &= \frac{1}{N_s}\sum_{k=1}^{K}\boldsymbol{h}_{ql}^{(k)}[n_s]\left(\boldsymbol{h}_{ql}^{(k)}[n_s]\right)^H + \sigma^2\boldsymbol{I}_{N_e}\end{aligned} \tag{28}$$

which is obtained by using relatively short-range average and, hence, channel-dependent. By contrast, for the Type-II.2 RMD/MS-MMSE MUD using relatively long-range channel average, the autocorrelation matrix is given by

$$\boldsymbol{R}_{\boldsymbol{y}_{ql}}[n_s] = \frac{1}{UN_s}\boldsymbol{C}[n_s]\boldsymbol{C}^T[n_s] + \sigma^2\boldsymbol{I}_{N_e} \tag{29}$$

In (27), the cross-correlation matrices for both the Type-II.1 and Type-II.2 are the same and given by

$$\boldsymbol{R}_{\boldsymbol{y}_{ql}\boldsymbol{v}_{ql}}[n_s] = \frac{1}{N_s}\boldsymbol{H}_{ql}[n_s] \tag{30}$$

Hence, when substituting (28) and (30) into (27), the weight matrix for the Type-II.1 RMD/MS-MMSE MUD is given by

$$\bar{\boldsymbol{W}}_{ql}[n_s] = \left(\boldsymbol{H}_{ql}[n_s]\boldsymbol{H}_{ql}{}^H[n_s] + N_s\sigma^2\boldsymbol{I}_{N_e}\right)^{-1}\boldsymbol{H}_{ql}[n_s] \tag{31}$$

which is dependent on the channels but independent subcarrier-by-subcarrier. When substituting (29) and (30) into (27), the weight matrix for the Type-II.2 RMD/MS-MMSE MUD is given by

$$\bar{\boldsymbol{W}}_{ql}[n_s] = \left(\frac{1}{U}\boldsymbol{C}[n_s]\boldsymbol{C}^T[n_s] + N_s\sigma^2\boldsymbol{I}_{N_e}\right)^{-1}\boldsymbol{H}_{ql}[n_s] \tag{32}$$

which is channel independent and also subcarrier independent.

Furthermore, when comparing (24) with (32), we can immediately find that the MMSE-MUDs used in the Type-I.2 and Type-II.2 RMD/MS-MMSE MUDs are the same. Hence, in the following discourse, only the name of Type I.2 is used.

*2) Reliability Measurement:* Upon following the analysis in [20], the reliabilities of the different CRUs can be measured in the principles of maximum likelihood (ML), after approximating the decision variables output by a corresponding MMSE-MUD as Gaussian random variables. First, for the Type-I RMD/MS-MMSE MUD, after approximating the decision variable $\hat{v}_q^{(k)}[n_s]$ as a Gaussian random variable, its mean and variance can be expressed as

$$\begin{aligned} E\left[\hat{v}_q^{(k)}[n_s]|v_q^{(k)}[n_s]\right] &= \left(\boldsymbol{w}_q^{(k)}[n_s]\right)^H\boldsymbol{h}_q^{(k)}[n_s]v_q^{(k)}[n_s] \\ \text{Var}\left[\hat{v}_q^{(k)}[n_s]\right] &= \left(\boldsymbol{w}_q^{(k)}[n_s]\right)^H\Big(\boldsymbol{R}_{\boldsymbol{y}_q}[n_s] \\ &\quad -\boldsymbol{h}_q^{(k)}[n_s]\left(\boldsymbol{h}_q^{(k)}[n_s]\right)^H/N_s\Big)\boldsymbol{w}_q^{(k)}[n_s]/2 \end{aligned} \tag{33}$$

where $\boldsymbol{w}_q^{(k)}[n_s] = \boldsymbol{R}_{\boldsymbol{y}_q}^{-1}[n_s]\boldsymbol{h}_q^{(k)}[n_s]/N_s$ is the $k$th column of $\boldsymbol{W}_q[n_s]$ given in (23). According to [20], the reliability of detecting $v_q^{(k)}[n_s]$ in ML sense can be expressed as

$$\begin{aligned} L_q^{(k)}[n_s] = \frac{1}{2\text{Var}\left[\hat{v}_q^{(k)}[n_s]\right]}\Bigg|\Bigg(2E\left[\hat{v}_q^{(k)}[n_s]|v_q^{(k)}[n_s] = \frac{1}{\sqrt{N_s}}\right] \\ -2E\left[\hat{v}_q^{(k)}[n_s]|v_q^{(k)}[n_s] = -\frac{1}{\sqrt{N_s}}\right]\Bigg)\hat{v}_q^{(k)}[n_s]\Bigg| \end{aligned} \tag{34}$$

The detection of $v_q^{(k)}[n_s]$ is rendered more reliable, when the value of $L_q^{(k)}[n_s]$ is bigger. Upon substituting (33) into (34) and carrying out some simplification as well as ignoring the irrelevant coefficients, we obtain

$$\begin{aligned} L_q^{(k)}[n_s] &= \left(1 - \frac{\left(\boldsymbol{h}_q^{(k)}[n_s]\right)^H\boldsymbol{R}_{\boldsymbol{y}_q}^{-1}[n_s]\boldsymbol{h}_q^{(k)}[n_s]}{N_s}\right)^{-1}|\hat{v}_q^{(k)}[n_s]| \\ &= \left(1 - \left(\boldsymbol{h}_q^{(k)}[n_s]\right)^H\boldsymbol{w}_q^{(k)}[n_s]\right)^{-1}|\hat{v}_q^{(k)}[n_s]| \end{aligned} \tag{35}$$

where $n_s = 0, 1, \ldots, N_s - 1$; $q = 1, 2, \ldots, Q$; $k = 1, 2, \ldots, K$. Equation (35) shows that, after $\boldsymbol{W}_q[n_s]$ is obtained, the reliabilities of the detections can be very easily evaluated.

For the Type-I.2 and Type-II.1 RMD/MS-MMSE MUDs, the corresponding reliabilities can be similarly obtained as above, which are given by

$$L_q^{(k)}[n_s] = \frac{\left[\sum_{l=1}^{L}\left(\boldsymbol{w}_{ql}^{(k)}[n_s]\right)^H\boldsymbol{h}_{ql}^{(k)}[n_s]\right] \times |\hat{v}_q^{(k)}[n_s]|}{\sum_{l=1}^{L}\left(\boldsymbol{w}_{ql}^{(k)}[n_s]\right)^H\left[\boldsymbol{R}_{\boldsymbol{y}_{ql}} - \frac{\boldsymbol{c}_k[n_s]\boldsymbol{c}_k^T[n_s]}{UN_sN_e}\right]\boldsymbol{w}_{ql}^{(k)}[n_s]} \tag{36}$$

for the Type-I.2 and

$$L_q^{(k)}[n_s] = \frac{\left[\sum_{l=1}^{L}\left(\boldsymbol{w}_{ql}^{(k)}[n_s]\right)^H\boldsymbol{h}_{ql}^{(k)}[n_s]\right]|\hat{v}_q^{(k)}[n_s]|}{\sum_{l=1}^{L}\left(\boldsymbol{w}_{ql}^{(k)}[n_s]\right)^H\left[\boldsymbol{R}_{\boldsymbol{y}_{ql}} - \frac{\boldsymbol{h}_{ql}^k[n_s]\left(\boldsymbol{h}_{ql}^k[n_s]\right)^H}{N_s}\right]\boldsymbol{w}_{ql}^{(k)}[n_s]} \tag{37}$$

for the Type-II.1, respectively. Note that, $\boldsymbol{R}_{\boldsymbol{y}_{ql}}$ in (36) is given by (29) and in (37) is given by (28). Correspondingly, $\boldsymbol{w}_{ql}^{(k)}[n_s]$ in (36) is given by (32) and in (37) is given by (31).

*3) RMD/MS-MMSE MUD Algorithm:* With the aid of the MMSE-MUDs and the RM as described above, we can now state the RMD/MS-MMSE MUD algorithms [20–22]. Since the RMD/MS-MMSE MUD algorithms for the Type-I.1, Type-II.1 and Type-I.2 are similar, they can be described together as follows.

**Initialization**: For $n_s = 0, 1, \ldots, N_s - 1$,

$$\boldsymbol{y}_a^{(0)}[n_s] = \boldsymbol{y}_a[n_s], \quad \boldsymbol{W}_a^{(0)}[n_s] = \boldsymbol{W}_a[n_s] \tag{38}$$

where $a$ is for $q$ or $ql$, $q = 1, 2, \ldots, Q$; $l = 1, 2, \ldots, L$.

**Detection**: for $i = 1, 2, ..., K$, carrying out the following operations:

1) *Forming decision variables*:

$$\hat{\boldsymbol{v}}_q^{(i)}[n_s] = \begin{cases} \left(\boldsymbol{W}_q^{(i-1)}[n_s]\right)^H\boldsymbol{y}_q^{(i-1)}[n_s], & \text{Type-I.1} \\ \sum_{l=1}^{L}\left(\boldsymbol{W}_{ql}^{(i-1)}[n_s]\right)^H\boldsymbol{y}_{ql}^{(i-1)}[n_s], & \text{Others} \end{cases} \tag{39}$$

2) *Determining and detecting the most reliable CRU*: For the CRUs, $k'_1, k'_2, ..., k'_{K-i+1}$, that have not been detected, computing their reliabilities according to the equations given in Section IV-A2, which are expressed as $L_q^{(k'_1)}[n_s], L_q^{(k'_2)}[n_s], \cdots, L_q^{(k'_{K-i+1})}[n_s]$, and identifying the most reliable user as

$$k_q^{(i)}[n_s] = \arg\max_{k'_t} \left\{ L_q^{(k'_1)}[n_s], \cdots, L_q^{(k'_{K-i+1})}[n_s] \right\} \tag{40}$$

whose decision variable is recorded and hard-decision of $\hat{V}_{qr_q}^{(k_q^{(i)}[n_s])}[n_s]$ is made.

3) *Interference cancellation*:

$$\begin{aligned} \boldsymbol{y}_a^{(i)}[n_s] =& \boldsymbol{y}_a^{(i-1)}[n_s] \\ & - \boldsymbol{h}_a^{(k_q^{(i)}[n_s])}[n_s] \hat{V}_{qr_q}^{(k_q^{(i)}[n_s])}[n_s]/\sqrt{N_s} \end{aligned} \tag{41}$$

where $\boldsymbol{h}_a^{(k_q^{(i)}[n_s])}[n_s]$ is the $k_q^{(i)}[n_s]$th column of $\boldsymbol{H}_a[n_s]$, corresponding to the CRU detected at the $i$th iteration of detection.

4) *Update*: Updating $\boldsymbol{W}_a^{(i-1)}[n_s]$'s to $\boldsymbol{W}_a^{(i)}[n_s]$'s.

In the above algorithm, $\boldsymbol{W}_a^{(i)}[n_s]$ can be updated from $\boldsymbol{W}_a^{(i-1)}[n_s]$ according to the formula [20]

$$\begin{aligned} \boldsymbol{W}_a^{(i)}[n_s] = \Bigg[ & \boldsymbol{W}_a^{(i-1)}[n_s] \\ & + \frac{\boldsymbol{w}_{a,k_q^{(i)}[n_s]}^{(i-1)}[n_s] \left( \boldsymbol{h}_a^{k_q^{(i)}[n_s]}[n_s] \right)^H \boldsymbol{W}_a^{(i-1)}[n_s]}{1 - \left( \boldsymbol{h}_a^{k_q^{(i)}[n_s]}[n_s] \right)^H \boldsymbol{w}_{a,k_q^{(i)}[n_s]}^{(i-1)}[n_s]} \Bigg] \boldsymbol{P}_a^{(i)}[n_s] \end{aligned} \tag{42}$$

for both the Type-I.1 and Type-II.1 RMD/MS-MMSE MUDs, while according to the formula

$$\begin{aligned} \boldsymbol{W}_a^{(i)}[n_s] = \Bigg[ & \boldsymbol{W}_a^{(i-1)}[n_s] \\ & + \frac{\frac{(\boldsymbol{R}_a^{(i-1)}[n_s])^{-1} \boldsymbol{c}_a^{k_q^{(i)}[n_s]}[n_s] \left( \boldsymbol{c}_a^{k_q^{(i)}[n_s]}[n_s] \right)^T \boldsymbol{W}_a^{(i-1)}[n_s]}{UN_s}}{1 - \frac{\left( \boldsymbol{c}_a^{k_q^{(i)}[n_s]}[n_s] \right)^T (\boldsymbol{R}_a^{(i-1)}[n_s])^{-1} \boldsymbol{c}_a^{k_q^{(i)}[n_s]}[n_s]}{UN_S}} \Bigg] \boldsymbol{P}_a^{(i)}[n_s] \end{aligned} \tag{43}$$

for the Type-I.2 RMD/MS-MMSE MUD. In the above two equations, $\boldsymbol{w}_{a,k_q^{(i)}[n_s]}^{(i-1)}[n_s]$ is the $k_q^{(i)}[n_s]$th column of $\boldsymbol{W}_a^{(i-1)}[n_s]$, $\boldsymbol{c}_a^{k_q^{(i)}[n_s]}[n_s]$ is the $k_q^{(i)}[n_s]$th column of $\boldsymbol{C}[n_s]$, while $\boldsymbol{P}_a^{(i)}[n_s]$ is a permutation matrix obtained from $\boldsymbol{I}_K$ by removing the columns corresponding to the CRUs detected.

### B. Orthogonal Demodulation and Inverse RNS Transform

After the fractional RMD/MS-MMSE MUDs, the estimates to the fractions of the orthogonal codes sent by the $k$th, $k = 1, 2, \ldots, K$, CRU can be expressed as

$$\hat{\boldsymbol{v}}_{qr_q}^{(k)} = \left[ \hat{v}_q^{(k)}[0], \hat{v}_q^{(k)}[1], \cdots, \hat{v}_q^{(k)}[N_s - 1] \right]^T \tag{44}$$

where $q = 1, 2, \ldots, Q$ and $\{\hat{v}_q^{(k)}[n]\}$ are the soft-values output by the MMSE-MUDs in the RMD/MS-MMSE MUD algorithms. Then, the MOSK demodulation [29] is carried out, which is constituted by $Q$ blocks with each responsible for recovering one of the $Q$ residues. Specifically, for the $q$th, $q = 1, 2, \ldots, Q$, block responsible for recovery of $r_q^{(k)}$, it first forms $m_q$ decision variables as

$$Z_{qm}^{(k)} = \Re \left\{ \sum_{n=0}^{N_s-1} \hat{v}_q^{(k)}[n] V_{qm}[n] \right\}, m = 0, 1, m_q - 1 \tag{45}$$

where $V_{qm}[n]$ is the $n$th fraction of the $m$th orthogonal code in the $q$th group, as shown in (5), for transmitting the $q$th residue. Then, the largest is selected from the decision variable set $\left\{ Z_{q0}^{(k)}, Z_{q1}^{(k)}, \cdots, Z_{q(m_q-1)}^{(k)} \right\}$ and the corresponding index of this largest term represents the estimate, expressed as $\hat{r}_q^{(k)}$, to $r_q^{(k)}$ of the $q$th residue transmitted by the $k$th CRU. Let the $Q$ estimates to the residues transmitted by the $k$th CRU be collected into

$$\hat{\boldsymbol{r}}^{(k)} = \left[ \hat{r}_1^{(k)}, \hat{r}_2^{(k)}, \cdots, \hat{r}_Q^{(k)} \right]^T, \ k = 1, 2, \ldots, K \tag{46}$$

Finally, $\hat{\boldsymbol{r}}^{(k)}$ is sent to the IRNST of Fig. 2, where the estimate $0 \leq \hat{X}_k < M$ to the transmitted message $X_k$ is obtained, for example, with the aid of the CRT [26]. Furthermore, when the RRNS is considered, $\hat{\boldsymbol{r}}^{(k)}$ represents the observations of a RRNS codeword [28]. In this case, the ratio statistic test (RST) assisted *erasure-only decoding*, *error-correction-only decoding* or the RST-assisted *error-and-erasure decoding* [27, 28] may be employed to decode $\hat{\boldsymbol{r}}^{(k)}$ and to recover the message $X_k$ transmitted.

### C. Characteristics of RRNS-Based MC/DS-CDDMA

From the analysis and discussion in the previous subsections, we can know that the RRNS MC/DS-CDDMA scheme has the following characteristics, when applied in CRs. First, the RRNS MC/DS-CDDMA is a multiple-access scheme of low complexity. In comparison with the conventional MMSE-MUD designed based on (17), which obtains the weight matrix from (18), Table I summarizes the number of operations required by the four detection schemes. In Table I, $a_1, \ a_2, \ \ldots, d'_1, \ d'_2$ are certain constants, when, $K$, the number of CRUs, is given. Furthermore, the column of 'Channel Dependence' indicates how the detection scheme is dependent on the channel knowledge. Specifically, the term of 'Auto/cross-correlation' corresponding to the first two detection schemes means that the invoked autocorrelation and cross-correlation matrices are dependent on the channel knowledge of all the subcarriers. The term of 'Subcarrier auto/cross-correlation' for the Type-II.1 MUD means that the invoked autocorrelation and cross-correlation matrices are only dependent on the channel knowledge of the subcarrier considered. By contrast, the term of 'Subcarrier cross-correlation' for the Type-I.2 MUD means that the related autocorrelation matrix is independent of channels, while the cross-correlation matrix is only dependent on the channel knowledge of the subcarrier considered. Finally, we note that the IC operations in the three proposed MUD schemes require the channel knowledge associated with all the subcarriers of the RRNS/MC DS-CDDMA system. From

TABLE I
COMPARISON OF THE NUMBER OF OPERATIONS REQUIRED BY THE VARIOUS DETECTION SCHEMES.

| Type | MMSE-MUD | SIC | Channel Dependence |
|---|---|---|---|
| **Conventional** | $a_1LN_e + a_2(LN_e)^2 + a_3(LN_e)^3$ | $-$ | Auto/cross-correlation |
| **Type I.1** | $b_1LN_e + b_2(LN_e)^2 + b_3(LN_e)^3$ | $b_1'KLN_e + b_2'(LN_e)^2$ | Auto/cross-correlation, IC |
| **Type II.1** | $c_1N_e + c_2N_e^2 + c_3N_e^3$ | $c_1'KN_e + c_2'N_e^2$ | Subcarrier auto/cross-correlation, IC |
| **Type I.2** | $d_1N_e + d_2N_e^2 + d_3N_e^3$ | $d_1'KN_e + d_2'N_e^2$ | Subcarrier cross-correlation, IC |

Table I, we can see that the Type-I.1 RMD/MS-MMSE MUD has a similar complexity as the conventional MMSE-MUD, both of which are proportional to $L^3N_e^3$ and expressed as $\mathcal{O}(L^3N_e^3)$. Both the Type-I.2 and Type-II.1 RMD/MS-MMSE MUDs have the complexity of $\mathcal{O}(N_e^3)$, since, in these two MUD schemes, the matrices need to be inverted are $(N_e \times N_e)$ dimensions. Furthermore, as shown in Section IV-A, in the Type I.2 and Type-II.1 RMD/MS-MMSE MUDs, the MMSE-MUDs are operated subcarrier-by-subcarrier independently. Additionally, the autocorrelation matrix used by the Type-I.2 RMD/MS-MMSE MUD is channel-free and, hence, it is not required to be updated, provided that the active CRUs do not change. When taken this into account, the complexity of the Type-I.2 RMD/MS-MMSE MUD is in fact only $\mathcal{O}(N_e^2)$.

Second, as our performance results in Section VI will show, although the complexity of the proposed three types of RMD/MS-MMSE MUDs is different, they are all highly promising MUD schemes, which are capable of achieving the near single-user error performance bound even a reasonable number of CRUs are supported. All the three proposed RMD/MS-MMSE MUDs outperform the MMSE-MUD in terms of the error performance.

Third, in the RRNS MC/DS-CDDMA systems, the MMSE-MUDs associated with the $U$ subcarriers can be implemented separately and independently. Hence, they are highly flexible and beneficial to reconfiguration in dynamic communication environments. For example, when some new PUs activate and occupy some of the subcarriers that the CRUs communicate on or when some other PUs complete their communications and release some subcarriers, the RRNS MC/DS-CDDMA system can readily adapt to these changes. It can simply terminate the communications on the subcarriers occupied by the new PUs without having to terminate the CRUs' communications. Furthermore, the RRNS MC/DS-CDDMA system may make use of the newly released subcarriers by the PUs for enhancing the communication performance.

Fourth, the RRNS MC/DS-CDDMA scheme is beneficial to PN sequence acquisition in dynamic communication environments. The studies in [17–19] show that the MC/DS-CDMA scheme is capable of providing advantages for PN sequence acquisition in comparison with the single-carrier DS-CDMA scheme. Furthermore, in the RRNS MC/DS-CDDMA, every CRU communicates using multiple subcarriers and the PN sequences on these subcarriers are synchronous. In this case, when there are new subcarriers added, the PN sequences used by the newly added subcarriers can be readily synchronized with the PN sequences of the existing subcarriers, without requiring the PN sequence acquisition procedure.

Moreover, the inherent properties of the RRNS make the RRNS MC/DS-CDDMA scheme highly robust and suitable for achieving seamless spectrum handoff in CR systems. According to the first property of the RNS arithmetic, the operations of the residues belonging to different moduli are mutually independent. Correspondingly, the operations with respect to different residues in Fig. 2 are independent. Therefore, the RRNS MC/DS-CDDMA scheme is highly flexible for reconfiguration. The second property of the RNS arithmetic explains that, if the RNS is designed with redundant moduli, forming the RRNS, some of the residues may be discarded without affecting recovery of result, provided that a sufficiently high dynamic range is retained by the reduced-range RRNS system. In this case, the RRNS MC/DS-CDDMA scheme is fault-tolerant.

In summary, all the above-mentioned properties of the RRNS MC/DS-CDDMA scheme are important for a multiple-access scheme operated in CR environments, which make the proposed RRNS MC/DS-CDDMA scheme a promising candidate for DMA in CR environments.

## V. PERFORMANCE ANALYSIS OF RRNS MC/DS-CDDMA SYSTEMS

In this section, we first analyze the outage probability of the RRNS MC/DS-CDDMA system. We assume that an outage occurs, when there are not sufficient subcarriers for the RRNS MC/DS-CDDMA system to be operated properly. Then, we analyze the lower bound error rate of the RRNS MC/DS-CDDMA system. Note that, it is extremely difficult to derive the expressions for the error rate of the RRNS MC/DS-CDDMA systems using our proposed RMD/MS-MMSE MUD. This is because, as shown in Section IV, the signals detected at different stages are at different reliability levels, and they are correlated too. Hence, for the RRNS/MC DS-CDDMA systems supporting multiple users (or CRUs), we use the Monte-Carlo simulation approaches to evaluate their BER performance.

### A. Outage Probability of RRNS MC/DS-CDDMA Systems

From Section II, we can readily know that the probability of the event that there are $U = C_P, 2C_P, ..., K_PC_P$ subchannels available for the CR system is

$$P_{idea}^{CR}(U) = P_{(K_P - \frac{U}{C_P})}, \tag{47}$$

when the CR system is operated under the ideal mode or is

$$P_{constraint}^{CR}(U) = \sum_{n=0}^{K_P - U/C_P} P_n P'_{(K_P - \frac{U}{C_P} - n)}, C_P \tag{48}$$

when it is operated under the spectrum handoff mode.

According to the principles of the RRNS MC/DS-CDDMA, when the RRNS$(Q,S)$ is employed, the RRNS MC/DS-CDDMA system requires at least $S$ number of subchannels for conveying $S$ out of the $Q$ number of residue digits, in order for the receiver to recover the transmitted message. Therefore, the outage probability is given by

$$\begin{aligned} P_{O,idea}^{CR}(S) =& \sum_{n=K_P-\lceil\frac{S}{C_P}\rceil+1}^{K_P} P_n \\ =& P_0 \sum_{n=K_P-\lceil\frac{S}{C_P}\rceil+1}^{K_P} \frac{K_P!}{(K_P-n)!n!}\left(\frac{\lambda}{\mu}\right)^n \end{aligned} \quad (49)$$

when the RRNS/MC DS-CDDMA system is operated under the ideal mode. In (49), $\lceil x \rceil$ returns the minimum integer larger than $x$ and $P_0$ is given in (1). By contrast, when operated under the handoff mode, the above outage probability is given by

$$\begin{aligned} P_{O,cons}^{CR}(S) =& P_{O,idea}^{CR} + \sum_{n=0}^{K_P-\lceil\frac{S}{C_P}\rceil}\left(P_n \sum_{i=K_P-n-\lceil\frac{S}{C_P}\rceil+1}^{K_P-n} P'_i\right) \\ =& P_{O,idea}^{CR} + P_0 e^{-\lambda K_P \Delta t} \sum_{i=K_P-\lceil\frac{S}{C_P}\rceil+1}^{K_P} \frac{(\lambda K_P \Delta t)^i}{i!} \\ &+ P_0 \sum_{n=1}^{K_P-\lceil\frac{S}{C_P}\rceil}\left[\frac{K_P!}{(K_P-n)!n!}\left(\frac{\lambda}{\mu}\right)^n e^{-\lambda(K_P-n)\Delta t}\right. \\ &\times \left.\sum_{k=K_P-n-\lceil\frac{S}{C_P}\rceil+1}^{K_P-n} \frac{(\lambda(K_P-n)\Delta t)^k}{k!}\right] \end{aligned} \quad (50)$$

where $\Delta t$ represents the duration of spectrum handoff, which is normalized by the symbol duration and takes integer value.

### *B. Error Performance Lower Bounds of RRNS MC/DS-CDDMA Systems*

According to [20, 22], the RMD/MS-MMSE MUD is usually capable of achieving the near single-user BER performance, even when the system is full-load, where full-load means that the number of users supported equals the spreading factor. Our simulation results in Section VI of this paper also show that the RRNS MC/DS-CDDMA systems employing the RMD/MS-MMSE MUD can also achieve promising performance that is close to the single-user BER performance, provided that $K \leq LN_e$ number of users are supported. Therefore, in this section, we analyze the error performance bound of the RRNS MC/DS-CDDMA systems by assuming that single user is supported, which represents the lower bound for the error performance of the RRNS MC/DS-CDDMA systems supporting multiple users. Furthermore, owing to the high efficiency of the RMD/MS-MMSE MUD, in most cases, the single-user error performance can be viewed as the approximate error performance of the RRNS MC/DS-CDDMA systems supporting multiple users.

When the RRNS MC/DS-CDDMA systems support single-user, all the three types of detection schemes considered in Section IV become the same and are equivalent to the matched-filtering (MF) detection. In the single-user case, the observation equation (15) in the context of the $q$th residue $r_q$ becomes

$$\begin{aligned} \boldsymbol{y}_{ql}[n_s] =& \frac{1}{\sqrt{U}}\boldsymbol{c}_k[n_s]h_{ql}^{(k)}[n_s]v_q^{(k)}[n_s] + \boldsymbol{n}_{ql}[n_s], \\ & l=1,2,\ldots,L;\ n_s=0,1,\ldots,N_s-1 \end{aligned} \quad (51)$$

where $\boldsymbol{n}_{ql}[n_s]$ is an $N_e$-length Gaussian noise vector with zero mean and a covariance matrix $\boldsymbol{I}_{N_e}/\gamma_s$. From (51), the $m_q$ decision variables can be formed using the MF principles as

$$\begin{aligned} Z_{qm} =& \Re\left\{\frac{\sqrt{U}}{\sum_{l=1}^{L}|h_{ql}^{(k)}|^2}\sum_{n_s=0}^{N_s-1}\frac{V_m[n_s]}{\sqrt{N_s}}\sum_{l=1}^{L}\left(h_{ql}^{(k)}\right)^*\boldsymbol{c}_k^T\boldsymbol{y}_{ql}[n_s]\right\}, \\ & m=0,1,\ldots,m_q-1 \end{aligned} \quad (52)$$

where $\sqrt{U}/\sum_{l=1}^{L}|h_{ql}^{(k)}|^2$ is applied to normalize the outputs. Without loss of any generality, let us assume that $r_q=0$ was transmitted. Then, when substituting (51) into the above equation, we obtain

$$\begin{aligned} Z_{q0} =& 1 + N_{q0} \\ Z_{qm} =& N_{qm}, m=1,2\ldots,m_q-1 \end{aligned} \quad (53)$$

where $N_{qm}$ is a Gaussian random variable with mean zero and variance $\sigma_{qm}^2 = U/(2\gamma_s\sum_{l=1}^{L}|h_{ql}^{(k)}|^2)$.

Let $\gamma_q = \bar{\gamma}_q\sum_{l=1}^{L}|h_{ql}|^2$ with $\bar{\gamma}_q = \gamma_s/U$ denoting the average SNR per subcarrier channel. Since each subcarrier channel is assumed to experience iid Rayleigh fading, $\gamma_q$ hence obeys the central $\chi^2$-distribution with $2L$ degrees of freedom, having the probability density function (PDF) [29]

$$f(\gamma_q) = \frac{1}{(L-1)!\bar{\gamma}_q^L}\gamma_q^{L-1}\exp\left(-\frac{\gamma_q}{\bar{\gamma}_q}\right), \gamma_q \geq 0 \quad (54)$$

Considering that $Z_{qm}$ is Gaussian distributed with a mean of one for $m=0$ and zero for $m \neq 0$ as well as a variance of $\sigma_{qm}^2$, we can obtain the PDF of $Z_{qm}$ by averaging its Gaussian PDF with respect to the PDF of (54), yielding

$$\begin{aligned} f_{Z_{q0}}(x) =& \frac{\sqrt{\bar{\gamma}_q}\Gamma(L+\frac{1}{2})}{\sqrt{\pi}(L-1)![1+\bar{\gamma}_q(x-1)^2]^{L+\frac{1}{2}}} \\ f_{Z_{qm}}(x) =& \frac{\sqrt{\bar{\gamma}_q}\Gamma(L+\frac{1}{2})}{\sqrt{\pi}(L-1)!(1+\bar{\gamma}_q x^2)^{L+\frac{1}{2}}},\ m=1,...,m_u-1 \end{aligned} \quad (55)$$

where $\Gamma(\cdot)$ represents the Gamma function [29]. Let us express the cumulative distribution function (CDF) of $Z_{qm},\ m \neq 0$, as

$$\begin{aligned} \mathcal{F}_{Z_{qm}}(y) =& \int_{-\infty}^{y} f_{Z_{qm}}(x)dx \\ =& \sqrt{\frac{\bar{\gamma}_q}{\pi}}\frac{\Gamma(L+\frac{1}{2})}{(L-1)!}\left[\frac{C_L(1)}{\sqrt{\bar{\gamma}_q}} + \sum_{l=1}^{L}\frac{C_L(l)y}{(1+\bar{\gamma}_q y^2)^{l-\frac{1}{2}}}\right] \end{aligned} \quad (56)$$

where, by definition,

$$C_L(l) = \frac{(2L-2)!!(2l-3)!!}{(2L-1)!!(2l-2)!!} \quad (57)$$

Then, the error probability of detecting the $q$th residue $r_q$ can be derived as [29]

$$\begin{aligned} P_e(m_q, L) &= 1 - \int_{-\infty}^{\infty}\left[\int_{-\infty}^{y} f_{Z_{qm}}(x)dx\right]^{m_q-1} f_{Z_{q0}}(y)dy \\ &= 1 - \int_{-\infty}^{\infty}\left[\mathcal{F}_{Z_{qm}}(y)\right]^{m_q-1} f_{Z_{q0}}(y)dy \\ &= (m_q-1)\int_{-\infty}^{\infty}\mathcal{F}_{Z_{qm}}(y-1)[\mathcal{F}_{Z_{qm}}(y)]^{m_q-2}d\mathcal{F}_{Z_{qm}}(y), \\ & q = 1, 2, \ldots, Q \end{aligned} \quad (58)$$

which can be evaluated by numerical integration.

When the RRNS MC/DS-CDMA is considered, where the total number of subcarriers $U$ is fixed, if all the $Q$ moduli are used exclusively for transmitting information, meaning that there are no redundant moduli, i.e., $Q = S$, then the transmitted RNS symbol $X_k$ is correctly received on the condition that all the $Q$ number of residue, $r_1, r_2, \ldots, r_Q$ are correctly received. Hence, the lower-bound of the average error probability of the RRNS/MC DS-CDMA systems can be expressed as [16]

$$P_{e,RNS}(Q, L) = 1 - \prod_{q=1}^{Q}[1 - P_e(m_q, L)] \quad (59)$$

When RRNS($Q, S$) coding, where $Q > S$, is invoked in our RRNS MC/DS-CDMA systems and when the 'error-correction only' decoding is employed, it can be shown that the lower-bound of the average error probability of the RRNS/MC DS-CDMA systems is given by [16]

$$\begin{aligned} P_{e,RRNS}(Q, L) =& 1 - \sum_{t=0}^{t_{max}}\left\{\sum_{\mathcal{N}\binom{Q}{t}}\left[\prod_{\substack{i=1 \\ q_1\neq q_2\neq\ldots\neq q_t}}^{t} P_e(m_{q_i}, L)\right.\right. \\ & \left.\left.\times\prod_{n=1, n\neq q_i}^{Q}(1 - P_e(m_n, L))\right]\right\} \end{aligned} \quad (60)$$

where $t_{max} = \lfloor (Q - S)/2 \rfloor$ represents the maximum number of errors that the RRNS($Q, S$) code can correct, and $\sum_{\mathcal{N}\binom{Q}{t}}$ represents all the possible selections that $t$ out of the $Q$ number of residues $\{\hat{r}_1, \hat{r}_2, ..., \hat{r}_Q\}$ are received in error. Furthermore, $P_e(m_n, L)$ in both (59) and (60) are given by (58).

Finally, when the RRNS MC/DS-CDDMA systems are considered, where the total number of subchannels $U$ is time-varying, the lower-bound error performance can be analyzed as follows. We assume that there is no information transmission in the CR system, if the number of available subchannels is lower than the minimum number of $S$ required by the RRNS MC/DS-CDDMA systems. In this case, we define

$$\begin{cases} f_L(U) = 1, \ f_Q(U) = U, \ \text{when } S \leq U \leq Q \\ f_L(U) = \lfloor \dfrac{U}{Q} \rfloor, \ f_Q(U) = Q, \ \text{when } Q < U \leq C \end{cases} \quad (61)$$

where $f_Q(U)$ and $f_L(U)$ represent the numbers of moduli used by the RRNS and the diversity order achieved, respectively, when there are $U$ number of subchannels available for the RRNS MC/DS-CDDMA systems. Additionally, in (61), $C$ is the total number of subchannels of the PR systems, as defined in Section II. Based on the above definitions, the lower-bound symbol error probability of the RRNS MC/DS-CDDMA systems operated in dynamic environments can be expressed as

$$P_{DMA} = \sum_{U=S}^{C} P_a^{CR}(U) P_{e,RRNS}\left(f_Q(U), f_L(U)\right) \quad (62)$$

where $P_a^{CR}(U)$ denotes the probability of $P_{ideal}^{CR}(U)$ given by (47) or the probability of $P_{constraint}^{CR}(U)$ given by (48), while $P_{e,RRNS}\left(f_Q(U), f_L(U)\right)$ is given by (60).

Let us below provide a range of performance results for characterizing the performance of the RRNS MC/DS-CDDMA systems.

## VI. Simulation Results and Discussion

In this section, we provide a number of figures to demonstrate the achievable performance of the RRNS MC/DS-CDMA and RRNS MC/DS-CDDMA systems employing the proposed MUDs, namely

- Type-I.1 RMD/MS-MMSE MUD;
- Type-I.2 RMD/MS-MMSE MUD;
- Type-II.1 RMD/MS-MMSE MUD.

The performance results shown in this section were all obtained from the C++ software tool called IT++. In our simulations, we assumed that random spreading sequences were employed for the DS spreading and that the subcarriers experienced independent frequency non-selective (flat) Rayleigh fading. For convenience, the parameters used for setting the PR and CR systems are summarized as follows.

- $C$: total number of subcarriers of the PR system;
- $K_P$: maximal number of PUs;
- $C_P$: number of subcarriers occupied by an active PU;
- $\lambda$, $1/\mu$ and $\lambda/\mu$: arrival rate of PUs, mean service time per active PU and *utilization factor*;
- $U$: total number of subcarriers used by the CR system;
- $Q$, $S$: total number of moduli and number of information moduli of the RRNS. Hence, the number of redundant moduli of the RRNS is $Q - S$;
- $L$: order of frequency diversity;
- $N_e = T_r/T_c$: number of chips per fraction of duration $T_r$;
- $K$: number of users (CRUs) supported by the CR systems;

In order to demonstrate and compare the error performance of our proposed three types of RMD/MS-MMSE MUDs, in Figs. 3 and 4, two RNS MC/DS-CDMA systems without using redundant moduli were studied, when assuming that the systems are operated in static communication environments. In the first RNS MC/DS-CDMA system considered for Fig. 3, we assumed that the system employed in total $U = 8$ subcarriers for transmitting $S = 2$ information moduli, $m_1 = 5$ and $m_2 = 7$, and achieving $L = 4$ orders of frequency diversity. We chose $M = 32$ and, hence, $B = \log_2 32 = 5$ bits were transmitted per symbol. In the RNS MC/DS-CDMA system considered for Fig. 4, we assumed that the system employed in total $U = 16$ subcarriers for transmitting $S = 4$ information

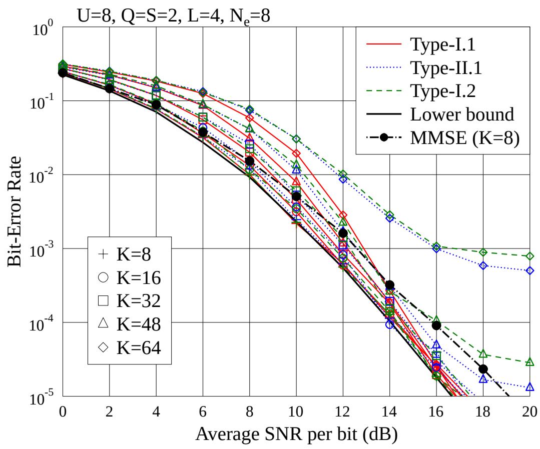


Fig. 3. BER versus average SNR per bit performance of the RNS-based MC/DS-CDMA systems employing $U = 8$ subcarriers, which convey $Q = S = 2$ residues attaining $L = 4$th order frequency diversity.

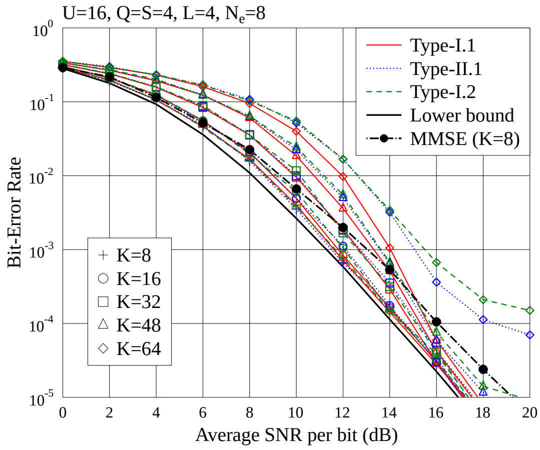


Fig. 4. BER versus average SNR per bit performance of the RNS-based MC/DS-CDMA systems employing $U = 16$ subcarriers, which convey $Q = S = 4$ residues attaining the $L = 4$th order frequency diversity.

moduli, $m_1 = 5$, $m_2 = 7$, $m_3 = 8$ and $m_4 = 9$, and also achieving $L = 4$ orders of frequency diversity. Correspondingly, we chose $M = 2048$ and every RNS symbol transmitted $B = \log_2 M = 11$ bits. In both the figures, the lower bound BER was depicted. Furthermore, in these two figures, the BER performance of the corresponding MC/DS-CDMA systems using MMSE-MUD to support $K = 8$ users is depicted. Figs. 3 and 4 explicitly show that any of the three proposed detection schemes outperforms the MMSE-MUD. As seen in Figs. 3 and 4, at a given SNR per bit, the Type-I.1, Type-I.2 or Type-II.1 RMD/MS-MUD may support significantly more CRUs than the MMSE-MUD, while attaining a similar BER. This observation becomes more declared, when the SNR per bit becomes higher. From Figs. 3 and 4, we observe that the Type-I.1 MUD outperforms both the Type-I.2 and Type-II.1 MUDs, while the Type-II.1 MUD outperforms the Type-I.2 MUD. This observation becomes more clear, either when the number of users supported increases, or when the average SNR per bit increases.

From Section IV-A1 we know that the MMSE-MUD invoked in the Type-I.1 RMD/MS-MMSE MUD carries out the joint detection of the signals transmitted on different subcarriers, which makes use of the channel knowledge about all the subcarriers. Correspondingly, as seen in Figs. 3 and 4, the Type-I.1 MUD is capable of achieving the near optimum BER performance that is close to the lower-bound (single-user BER), even when the number of users supported is as high as $K = 2N_eL = 64$. Furthermore, as shown in Figs. 3 and 4, the BER of the Type-I.1 MUD converges to the lower-bound as the average SNR increases. By contrast, as the analysis in Section IV-A1 shows, the MMSE-MUD invoked in the Type-II.1 and Type-I.2 MUDs detects each subcarrier signal separately. The difference between the MMSE-MUDs used in the Type-II.1 and Type-I.2 MUDs is that the autocorrelation matrix in the the MMSE-MUD for the Type-II.1 requires real-time channel knowledge, while that for the Type-I.2 is independent of channel knowledge. Hence, these two MUDs have a degraded capability of MUI suppression, in comparison with the Type-I.1 MUD. Therefore, as observed in Figs. 3 and 4, the BER curves of these two MUDs diverge from the lower-bound, when the number of users supported is relatively high, such as $K = 32$ or $64$ in Fig. 3 and $K = 64$ in Fig. 4. However, when the number of users supported is not very high, typically, when $K \leq LN_e$, or when the operational average SNR is relatively low, such as, yielding a BER of about $0.01$, the performance of the proposed three types of MUDs is usually close to each other, with the difference typically within $0.5$ dB (the only exception is the case of $K = 64$ in Fig. 3).

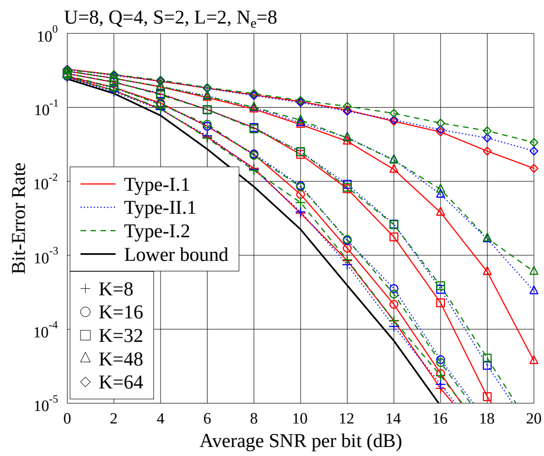


Fig. 5. BER versus average SNR per bit performance of the RRNS MC/DS-CDMA systems communicating over frequency-selective Rayleigh fading channels.

Figs. 5 and 6 illustrate the BER performance of the RRNS MC/DS-CDMA systems employing the proposed MUDs, when non-dynamic communication environments were assumed. In the context of these two figures, RRNS schemes were considered. Specifically, for Fig. 5, the RRNS$(4, 2)$ was used, where the two information moduli were $m_1 = 5, m_2 = 7$ and the two redundant moduli were $m_3 = 8, m_4 = 9$. By contrast, for Fig. 6, the RRNS$(8, 4)$ was employed, where the four information moduli were $m_1 = 5, m_2 = 7, m_3 =$

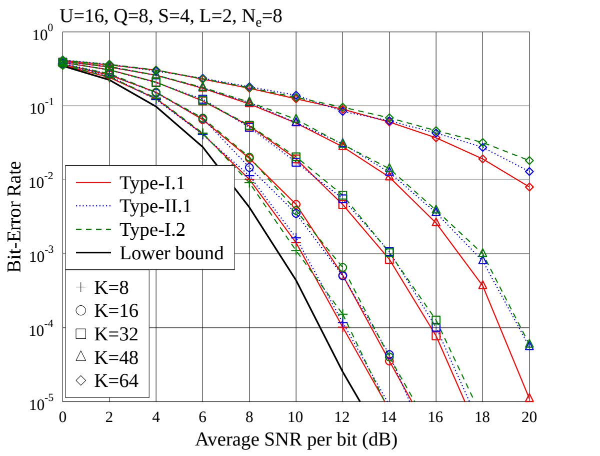


Fig. 6. BER versus average SNR per bit performance of the RRNS MC/DS-CDMA systems communicating over frequency-selective Rayleigh fading channels.

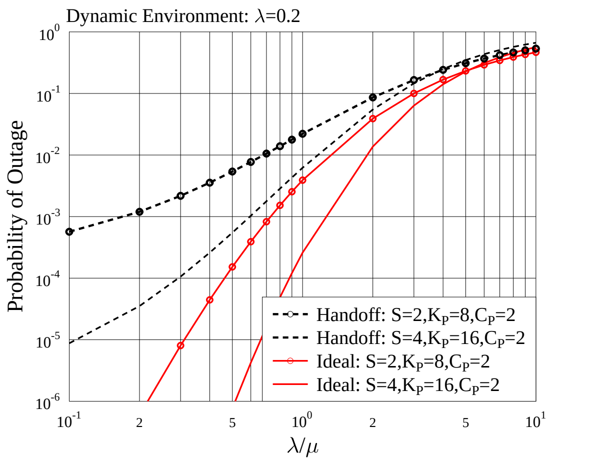


Fig. 7. Outage probability versus $\lambda/\mu$ (utilization factor) performance of the RRNS MC/DS-CDDMA systems using two information moduli and two redundant moduli and $\Delta t = 1$.

$8, m_4 = 9$, while the four redundant moduli were $m_5 = 11, m_6 = 13, m_7 = 17, m_8 = 19$. The value of $M$ was chosen as $M = 32$ for Fig. 5 and as $M = 2048$ for Fig. 6. Furthermore, as for Figs. 3 and 4, the impact of the number of users was evaluated, when the proposed three types of MUD schemes were employed, respectively.

From the results of Figs. 5 and 6, we observe that, within the considered SNR region, the BER performance achieved by the three types of MUDs for the various number users is very similar. This observation explains that the Type-II.1 and, especially, Type-I.2, which are suitable for implementation in dynamic environments, are also promising MUDs in terms of the BER performance. When we compare the results in Figs. 5 and 6, where RRNS was considered and $L = 2$ orders of diversity were used, with that in Figs. 3 and 4, where no RRNS was used but $L = 4$ orders of diversity were achieved, we can observe that the BER performance shown in Figs. 3 and 4 is generally better than the corresponding BER performance shown in Figs. 5 and 6. The reason for this observation is that, in this paper, hard-decision based RRNS decoding is assumed and, furthermore, the RRNS codes used are relatively short, with RRNS$(4, 2)$ for Fig. 5 and RRNS$(8, 4)$ for Fig. 6. Consequently, the decoding scheme is outperformed by the diversity scheme within the SNR region considered. Note that, the error performance of the RRNS codes may be significantly improved, when soft-decision based decoding scheme is used.

Fig. 7 shows the outage probability of the RRNS MC/DS-CDDMA system in the dynamic communication environments, where the PR system was configured by the parameters shown in the figure. Both the ideal mode and handoff mode were evaluated. Two information moduli and two redundant moduli were employed by the RRNS. The results of Fig. 7 explicitly show that the performance predicted without taking into account of spectrum handoff may be too optimistic, especially, when the utilization factor $\lambda/\mu$ of the PR system is relatively low. Additionally, given a fixed utilization factor, the results of Fig. 7 show that the outage performance of the RRNS MC/DS-CDDMA system improves as the total number of subbands of the PR system increases, even when the number of PUs supported increases proportionally with the subbands.

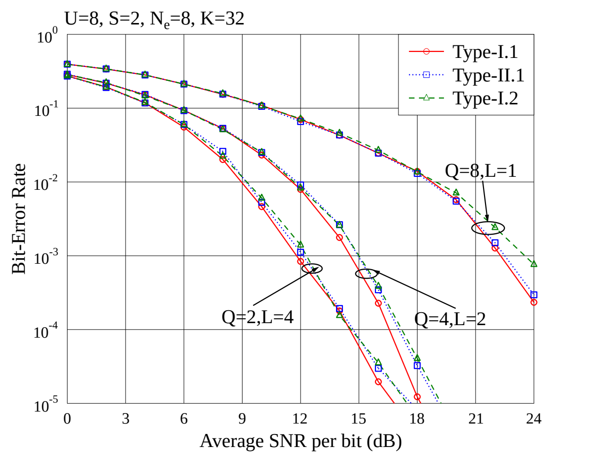


Fig. 8. BER versus average SNR per bit performance of the RRNS MC/DS-CDMA systems communicating over frequency-selective Rayleigh fading channels.

In Figs. 8 and 9, we compare the BER performance of the RRNS MC/DS-CDMA systems, when various number of redundant moduli and various order of frequency diversity are used, while maintaining the total number of subcarriers, i.e., $U = QL$, a constant. As the results in Figs. 8 and 9 show, the BER performance of the RRNS MC/DS-CDMA systems improves, as the value of $L$ increases and the value of $Q$ decreases. This observation implies that, when hard-decision based RRNS decoding is employed, obtaining frequency diversity, which is equivalent to using repetition code with soft combining, is more beneficial than using redundant moduli for error correction. Note that, soft-decision based RRNS decoding is beyond the consideration of the current paper. However, we note that the BER performance of the RRNS MC/DS-CDMA systems should be significantly improved, when the soft-decision based RRNS decoding is employed.

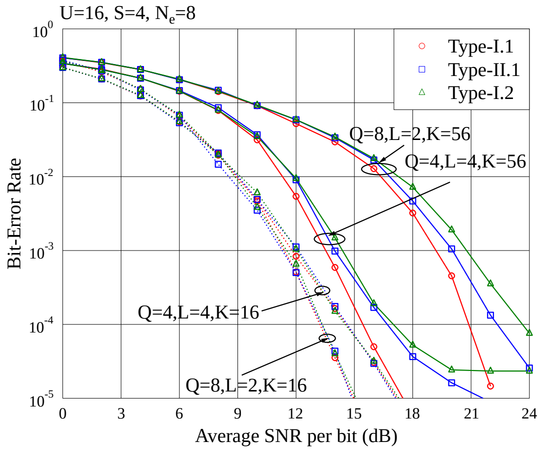


Fig. 9. BER versus average SNR per bit performance of the RRNS MC/DS-CDMA systems communicating over frequency-selective Rayleigh fading channels.

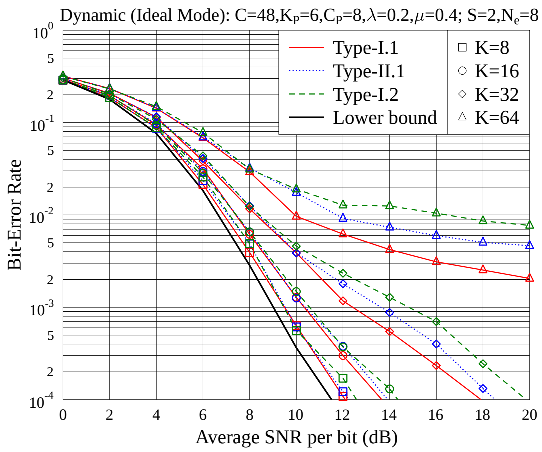


Fig. 10. BER versus average SNR per bit performance of the RRNS MC/DS-CDDMA systems communicating over frequency-selective Rayleigh fading channels, where the RRNS has $S = 2$ information moduli and upto $Q-S = 4$ redundant moduli.

In Figs. 10 and 11, we investigate the BER performance of the RRNS MC/DS-CDDMA systems employing, respectively, the proposed three types of MUDs, when communicating over dynamic spectrum environments. In Fig. 10, we assumed that the CR system was operated under the ideal mode, while in Fig. 11, we assumed that the CR system was operated under the handoff mode. For both the figures, the PR systems were structured by the parameters $C = 48$, $K_p = 6$, $C_p = 8$, $\lambda = 0.2$ and $\mu = 0.4$. The CR systems were assumed to use $S = 2$ information moduli, namely, $m_1 = 5, m_2 = 7$, and upto $Q - S = 4$ redundant moduli, which were $m_3 = 8, m_4 = 9, m_5 = 11, m_6 = 13$. From the results of Figs. 10 and 11, we observe that, when the number of CRUs supported is relatively low, such as $K \leq 2N_e$, the BER performance of the RRNS MC/DS-CDDMA systems using any of the proposed MUDs is close to the lower BER bound. However, as the number of CRUs supported increases, the BER performance of the RRNS MC/DS-CDDMA systems degrades. Furthermore, as shown in Fig. 11 corresponding to the handoff mode, BER error-floors

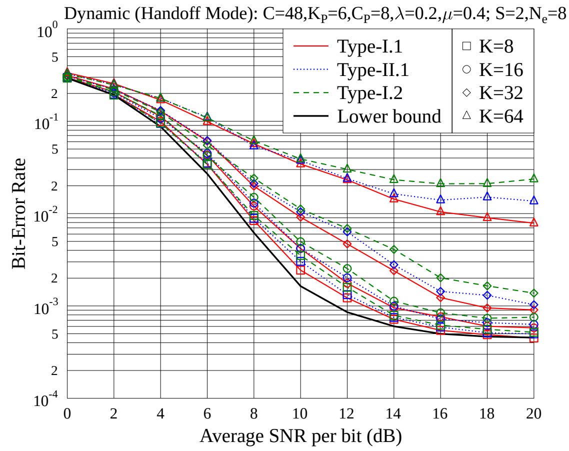


Fig. 11. BER versus average SNR per bit performance of the RRNS MC/DS-CDDMA systems communicating over frequency-selective Rayleigh fading channels, where the RRNS has $S = 2$ information moduli and upto $Q-S = 4$ redundant moduli and $\Delta t = 1$.

are observed, even when single CRU is supported. In contrast, when operated under the ideal mode, as shown in Fig. 10, error floors are observed only for the cases of $K = 64$. The reason for the observation of error floors in Fig. 11 is that, under the handoff mode, the transmission on some subcarriers has to be terminated, once the subcarriers are required by PUs. In this case, the CRBS has to detect the transmitted signals based on the incompletely received signals, yielding high error rate detection.

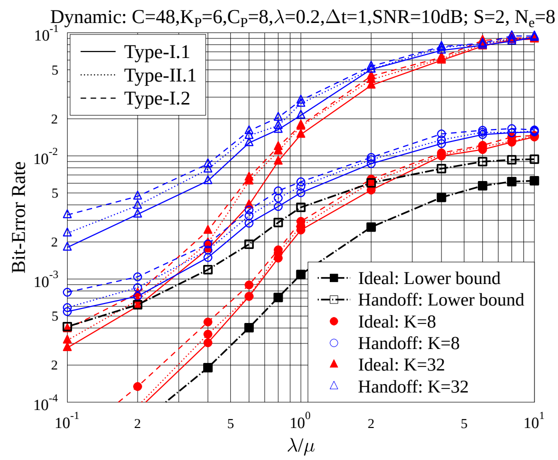


Fig. 12. BER versus $\lambda/\mu$ (utilization factor) performance of the RRNS MC/DS-CDDMA systems communicating over frequency-selective Rayleigh fading channels, where the RRNS has $S = 2$ information moduli and upto $Q - S = 4$ redundant moduli.

Fig. 12 shows the BER performance of the RRNS MC/DS-CDDMA systems against the utilization factor, $\lambda/\mu$, of the PR systems. From the results, we can observe that the BER increases, as the utilization factor of the PR systems increases, which results in less subcarriers for operation of the RRNS MC/DS-CDDMA systems. Again, as shown in Fig. 12, the BER performance predicted based on the ideal mode is over optimistic in contrast to that predicted based on the more practical handoff mode.

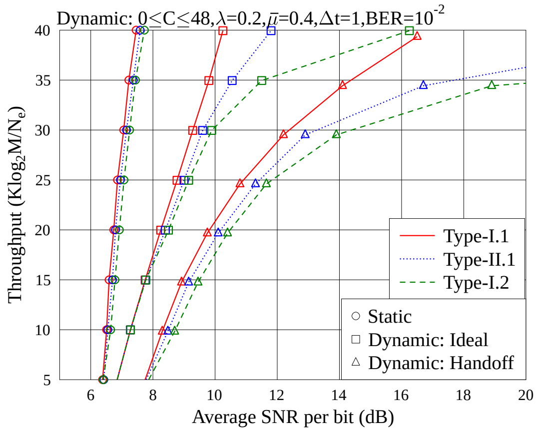


Fig. 13. Throughput versus average SNR per bit performance of the RRNS MC/DS-CDDMA systems communicating over frequency-selective Rayleigh fading channels.

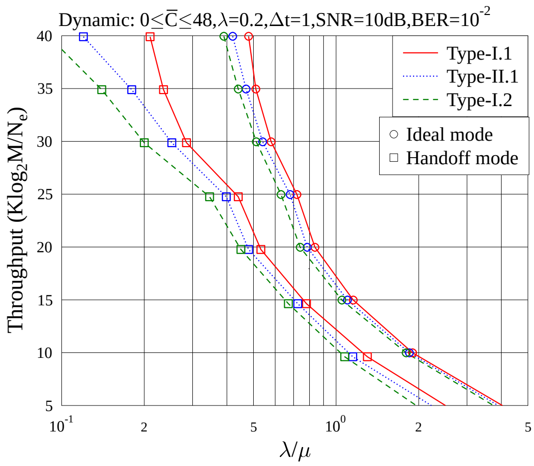


Fig. 14. Throughput versus $\lambda/\mu$ (utilization factor) performance of the RRNS MC/DS-CDDMA systems communicating over frequency-selective Rayleigh fading channels.

Finally, in Figs. 13 and 14, we evaluate the throughput that the RRNS MC/DS-CDDMA CR systems are able to achieve. In Fig. 13, the *static environment* corresponds to the RRNS MC/DS-CDDMA CR systems communicating using all the $C$ subcarriers. By contrast, the dynamic environment is explained by the parameters $0 \leq \bar{C} \leq 48, \lambda = 0.2, \mu = 0.4$ for the PR systems. When operated in the dynamic environment, both the ideal mode and handoff mode were considered, respectively. In these two figures, the throughput depicted was evaluated as follows. Given the BER required, the maximum number of CRUs supportable is first identified. Then, the throughput of the RRNS MC/DS-CDDMA system is calculated as $(K \times \log_2 M)/N_e$. From the results of Fig. 13, we can observe that, at a given average SNR per bit, the throughput of the systems operated under the static environments is significantly higher than that of the systems operated under the dynamic environments. When operated under the dynamic environments, the throughput predicted by assuming the ideal mode is explicitly higher than that predicted by assuming the handoff mode. The results of Fig. 14 show that, for both the ideal mode and the handoff mode, the throughput of the RRNS MC/DS-CDDMA system decreases, as the load of the PR system becomes heavier, i.e., as the utilization factor $\lambda/\mu$ increases.

## VII. Conclusions

In this paper, we have proposed a RRNS MC/DS-CDDMA scheme for dynamic access of the frequency spectrums in CRs. Along with the RRNS MC/DS-CDDMA, three types of MUD schemes, namely, the Type-I.1, Type-I.2 and Type-II.1 RMD/MS-MMSE MUDs, have been proposed. The error and throughput performance of the RRNS MC/DS-CDDMA systems have been investigated by assuming communications over frequency-selective fading channels and that the PUs activate according to a Poisson process. From our studies and performance results, we may conclude that the RRNS MC/DS-CDDMA constitutes one of the highly promising DMA scheme for application in CRs. First, with the aid of the proposed low-complexity MUDs, the RRNS MC/DS-CDDMA is capable of accommodating a substantial number of CRUs and still achieving near single-user error performance. Second, benefited from the MC/DS-CDMA and the subcarrier-by-subcarrier independent MMSE-MUD in the Type-I.2 or Type-II.1 RMD/MS-MMSE MUD, the RRNS MC/DS-CDDMA is well suitable for operation in the CRs environments. Furthermore, owing to the properties of the MC/DS-CDMA, RRNS and the proposed Type-I.2 or Type-II.1 RMD/MS-MMSE MUD, in the RRNS MC/DS-CDDMA systems, new spectrums can be readily added to the CR system and the spectrums found to be occupied by the PRs can be simply switched off, without having to break the communications. In other words, the RRNS MC/DS-CDDMA is capable of implementing seamless access and achieving smooth handoff between different spectrums, with the aid of only simple spectrum control and spectrum allocation protocols.

## Acknowledgment

This work was supported in part by the National Basic Research Program of China (973 Program, Grant No. 2010CB731803) and National Science Foundation for Innovative Research Groups of China (grant no. 60921001). It was also carried out in the framework of COST Action IC0905 “TERRA”.

## References


[1] W. Zhang and K. B. Letaief, “Cooperative spectrum sensing with transmit and relay diversity in cognitive radio networks,” *IEEE Trans. on Wireless Comm.*, vol. 7, no. 12 Part 1, pp. 4761–4766, 2008.

[2] J. Mitola III and G. Q. Maguire Jr, “Cognitive radio: making software radios more personal,” *IEEE personal Comm.*, vol. 6, no. 4, pp. 13–18, 1999.

[3] F. C. Commission, “Notice of proposed rule making and order: Facilitating opportunities for flexible, efficient, and reliable spectrum use employing cognitive radio technologies,” *ET Docket No. 03-108*, Feb. 2005.

[4] I. F. Akyildiz, W. Y. Lee, M. C. Vuran, and S. Mohanty, "NeXt generation/dynamic spectrum access/cognitive radio wireless networks: a survey," *Computer Networks*, vol. 50, no. 13, pp. 2127–2159, 2006.

[5] T. Yucek and H. Arslan, "A survey of spectrum sensing algorithms for cognitive radio applications," *IEEE Comm. Surveys and Tutorials*, vol. 11, no. 1, pp. 116–130, 2009.

[6] A. Goldsmith, S. A. Jafar, I. Maric, and S. Srinivasa, "Breaking spectrum gridlock with cognitive radios: An information theoretic perspective," *Proc. of the IEEE*, vol. 97, no. 5, pp. 894–914, 2009.

[7] S. Zhang, L.-L. Yang, and Y. Zhang, "Redundant residue number system based multicarrier DS-CDMA for dynamic multiple-access in cognitive radios," in *IEEE VTC2011-Spring*, Budapest, Hungary, 15 - 18 May 2011.

[8] L.-L. Yang and L. Hanzo, "Multicarrier DS-CDMA: a multiple access scheme for ubiquitous broadband wireless communications," *IEEE Comm. Mag.*, vol. 41, no. 10, pp. 116–124, 2003.

[9] L.-L. Yang and L. Hanzo, "Software-defined-radio-assisted adaptive broadband frequency hopping multicarrier DS-CDMA," *IEEE Comm. Mag.*, vol. 40, no. 3, pp. 174–183, 2002.

[10] L.-L. Yang and L.-C. Wang, "Zero-forcing and minimum mean-square error multiuser detection in generalized multicarrier DS-CDMA systems for cognitive radio," *EURASIP J. on Wireless Comm. and Net.*, vol. 2008, pp. 1–13, 2008.

[11] L.-L. Yang, *Multicarrier Communications*. John Wiley & Sons, 2009.

[12] R. W. Watson and C. W. Hastings, "Self-checked computation using residue arithmetic," *Proc. of the IEEE*, vol. 54, no. 12, pp. 1920–1931, 1966.

[13] N. S. Szabo and R. I. Tanaka, *Residue arithmetic and its applications to computer technology*, 1967.

[14] E. D. Di Claudio, G. Orlandi, and F. Piazza, "A systolic redundant residue arithmetic error correction circuit," *IEEE Trans. on Computer*, vol. 42, pp. 427–432, 1993.

[15] L.-L. Yang and L. Hanzo, "Performance of residue number system based DS-CDMA over multipath fading channels using orthogonal sequences," *European Trans. on Telecomm.*, vol. 9, no. 6, pp. 525–535, 1998.

[16] L. Hanzo, L.-L. Yang, E. L. Kuan, and K. Yen, *Single-and Multi-Carrier DS-CDMA: Multi-user Detection, Space-Time Spreading, Synchronisation, Networking, and Standards*. John Wiley & Sons, 2003.

[17] D. Lee and L. B. Milstein, "Analysis of a multicarrier DS-CDMA code-acquisition system," *IEEE Trans. on Comm.*, vol. 47, no. 8, pp. 1233–1244, Aug. 1999.

[18] L.-L. Yang and L. Hanzo, "Parallel code-acquisition for multicarrier DS-CDMA systems communicating over multipath Nakagami fading channels," in *Proc. of IEEE GLOBECOM'2000*, San Francisco, California, November 27 - Dec. 1 2000.

[19] L.-L. Yang and L. Hanzo, "Serial acquisition performance of single- and multi-carrier DS-CDMA over Nakagami-$m$ fading channels," *IEEE Trans. on Wireless Comm.*, vol. 1, no. 4, pp. 692–702, Oct. 2002.

[20] L.-L. Yang, "Receiver multiuser diversity aided multi-stage minimum mean-square error detection for heavily loaded DS-CDMA and SDMA systems," *IEEE Trans. on Comm.*, vol. 56, no. 12, pp. 3397–3404, 2010.

[21] L.-L. Yang, "Using multi-stage MMSE detection to approach optimum error performance in multiantenna MIMO systems," in *IEEE VTC 2009-Fall*. IEEE, 2009, pp. 1–5.

[22] L.-L. Yang, "Receiver multiuser diversity aided multi-stage MMSE multiuser detection: A low-complexity detector fast-converging to the optimum," in *IEEE VTC 2010-Spring*. IEEE, 2010, pp. 1–5.

[23] L.-L. Yang, "Receiver multiuser diversity aided multi-stage MMSE multiuser detection for DS-CDMA and SDMA systems employing I-Q modulation," in *IEEE VTC 2010-Fall*. IEEE, 2010, pp. 1–5.

[24] D. G. Kendall, "Stochastic processes occurring in the theory of queues and their analysis by the method of the embedded Markov chain," *The Annals of Mathematical Statistics*, vol. 24, no. 3, pp. 338–354, 1953.

[25] D. P. Bertsekas and R. Gallager, *Data Networks (2nd Ed.)*. Prentice-hall Englewood Cliffs, NJ, 1992.

[26] H. Krishna and J. D. Sun, "On theory and fast algorithms for error correction in residue number system product codes," *IEEE Trans. on Computers*, vol. 42, no. 7, p. 853, 1993.

[27] L.-L. Yang and L. Hanzo, "Ratio statistic test assisted residue number system based parallel communication systems," in *Proc. of IEEE VTC'99*, 1999, pp. 894–898.

[28] L.-L. Yang and L. Hanzo, "Minimum-distance decoding of redundant residue number system codes," in *IEEE Int. Conf. on Comm.*, 2001, pp. 2975–2979.

[29] J. G. Proakis, *Digital Communications*. McGraw-Hill, 1995.

[30] L.-L. Yang and L. Hanzo, "Performance of generalized multicarrier DS-CDMA over Nakagami-$m$ fading channels," *IEEE Trans. on Comm.*, vol. 50, no. 6, pp. 956–966, 2002.

[31] B. Steiner, "Time domain uplink channel estimation in multicarrier-CDMA mobile radio system concepts," in *Multi-Carrier Spread-Spectrum*, K. Fazel and G. P. Fettweis, Eds. Kluwer Academic Publishers, 1997, pp. 153–160.

[32] P. Hoeher, S. Kaiser, and P. Robertson, "Pilot-symbol-aided channel estimation in time and frequency," in *Multi-Carrier Spread-Spectrum*, K. Fazel and G. P. Fettweis, Eds. Kluwer Academic Publishers, 1997, pp. 169–178.

[33] N. Eshima and T. Kohda, "Statistical approach to the code acquisition problem in direct-sequence spread-spectrum communication systems," *IMA J. of Math. Control and Inf.*, vol. 23, no. 2, pp. 149–163, 2006.

[34] N. Eshima, T. Kohda, and M. Tabata, "Statistical solution to the capacity problem in direct-sequence code-division multiple access communication systems," *IMA J. of Math. Control and Inf.*, vol. 24, no. 3, pp. 289–298, 2007.

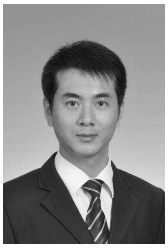

**Zhang Shuo received his B.Eng. degree in Microelectronics from Shandong University, Jinan, China, in 2006. Since 2006, he has been pursuing his Ph.D. degree in the School of Electronics and Information Engineering, Beihang University. From Sep. 2009 to Oct. 2010, he was a visiting Ph.D. student to the School of Electronics and Computer Science, University of Southampton, United Kingdom. His research interests include multicarrier systems, multiuser detection and dynamic multiple-access in cognitive radios.**

**Lie-Liang Yang (M'98, SM'02) received his BEng degree in communications engineering from Shanghai TieDao University, Shanghai, China in 1988, and his MEng and PhD degrees in communications and electronics from Northern (Beijing) Jiaotong University, Beijing, China in 1991 and 1997, respectively. From June 1997 to December 1997 he was a visiting scientist of the Institute of Radio Engineering and Electronics, Academy of Sciences of the Czech Republic. Since December 1997, he has been with the University of Southampton, United Kingdom, where he is the professor of wireless communications in the School of Electronics and Computer Science. Dr. Yang's research has covered a wide range of topics in wireless communications, networking and signal processing. He has published over 270 research papers in journals and conference proceedings, authored/co-authored three books and also published several book chapters. The details about his publications can be found at http://www-mobile.ecs.soton.ac.uk/lly/. He is currently an associate editor to the *IEEE Trans. on Vehicular Technology*, *Journal of Communications and Networks* (JCN) and the *Security and Communication Networks (SCN) Journal*.**

**Youguang Zhang received his B.Sc. and M.Sc. degrees in mathematics from Zhejiang Normal University, Jinghua, China, in 1984, and Peking University, Beijing, China, in 1987, respectively, and his Ph.D degree in electronics from Biehang University, Beijing, China, in 1990. Since September 1990, he has been with the School of Electronics and Information Engineering, Beihang University, Beijing, China, and currently holds an academic post of Professor. His research interests include broadband wireless communications, cognitive radio (CR), and signal processing.**